

# Metal sorption to ferrihydrite

Phosphate effects, X-ray absorption spectroscopy and  
surface complexation modelling

Charlotta Tiberg

*Faculty of Natural Resources and Agricultural Science  
Department of Soil and Environment  
Uppsala*

Doctoral Thesis  
Swedish University of Agricultural Sciences  
Uppsala 2016

Acta Universitatis agriculturae Sueciae

2016:56

ISSN 1652-6880

ISBN (print version) 978-91-576-8614-5

ISBN (electronic version) 978-91-576-8615-2

© 2016 Charlotta Tiberg, Uppsala

Print: SLU Service/Repro, Uppsala 2016

# Metal sorption to ferrihydrite. Phosphate effects, X-ray absorption spectroscopy and surface complexation modelling

## Abstract

Phosphorus affects the sorption of many metals and arsenate to iron (hydr)oxides. This may influence the mobility and bioavailability of metals and arsenate in soil and water. Phosphorus therefore plays an important role in, *e.g.*, determining the ecotoxicological risk of contaminants in soils.

The overall aim of this thesis was to improve the understanding of lead(II), copper(II), cadmium(II) and arsenate binding to iron (hydr)oxides. The focus was on how phosphate affects the sorption on ferrihydrite and in soils where ferrihydrite is an important constituent.

The effect of phosphate on the sorption of lead(II), copper(II), cadmium(II) and arsenate was determined by batch experiments. X-ray absorption spectroscopy (XAS) was performed to identify the binding mechanisms. Geochemical models were developed based on the XAS results and knowledge about the mineral or soil properties.

Phosphate enhanced the sorption of lead(II), copper(II) and cadmium(II) to ferrihydrite. The increased sorption was best explained by the formation of ternary complexes including the ferrihydrite surface, the metal and the phosphate ion. Phosphate competed strongly with arsenate for sorption sites on ferrihydrite. The competition was even stronger on poorly crystalline aluminium hydroxide.

Zero-valent iron that is mixed into soil rapidly oxidises to ferrihydrite that can adsorb contaminants. It was shown that the immobilisation of copper and arsenic in soils that had been stabilised by zero-valent iron is long-lasting. Copper immobilisation was most effective at high pH (>6) and at low organic matter content. Competition with phosphate needs to be taken into account when modelling arsenate sorption in soils. Otherwise arsenate sorption may be greatly overestimated.

Metal sorption to some podzolised soils was investigated in batch experiments. Despite the large influence on metal sorption in the pure ferrihydrite systems the addition of phosphate did not affect lead(II), copper(II) or cadmium(II) sorption to the B and C horizons of podzolised soils. The reasons may be strong metal binding to organic matter combined with a relatively small addition of phosphorus in the experiments.

In conclusion this thesis shows that phosphate greatly affects the sorption of lead(II), copper(II), cadmium(II) and arsenate to iron (hydr)oxides. To determine the impact of this effect in more complex matrices such as soils, more research is needed.

*Keywords:* Lead, copper, cadmium, arsenate, phosphate, ferrihydrite, iron (hydr)oxide, aluminium hydroxide, zero-valent iron, sorption, surface complexation modelling, EXAFS spectroscopy

*Author's address:* Charlotta Tiberg, SLU, Department of Soil and Environment,  
P.O. Box 7014, 750 07 Uppsala, Sweden  
*E-mail:* Charlotta.Tiberg@slu.se

# Contents

<b>List of Publications</b>	<b>7</b>
<b>Abbreviations</b>	<b>9</b>
<b>1 Introduction</b>	<b>11</b>
<b>2 Aim</b>	<b>13</b>
2.1 Overall aim	13
2.2 Specific objectives	13
<b>3 Background</b>	<b>15</b>
3.1 Iron and aluminium (hydr)oxides	15
3.1.1 Ferrihydrite	16
3.1.2 Mixtures of iron and aluminium (hydr)oxides	17
3.2 Sorption of lead(II), copper(II) and cadmium(II) to ferrihydrite	17
3.2.1 Sorption in single sorbate systems	17
3.2.2 Sorption in ternary systems	19
3.3 Sorption of arsenate and phosphate to ferrihydrite and poorly crystalline aluminium hydroxide	20
3.3.1 Sorption in single sorbent systems	20
3.3.2 Sorption to mixed sorbents	22
3.4 Partitioning of elements in soil	23
3.4.1 Using iron (hydr)oxides for immobilisation of metals and arsenic in soils	24
<b>4 Materials and methods</b>	<b>25</b>
4.1 Overview of the experimental work	25
4.2 Characterisation of minerals and soils	26
4.3 Batch experiments	26
4.3.1 Batch experiments with ferrihydrite and aluminium hydroxide	26
4.3.2 Batch experiments with soils	28
4.4 X-ray absorption spectroscopy	29
4.4.1 X-ray absorption near edge structure	30
4.4.2 Extended x-ray absorption fine structure	30
4.5 Geochemical modelling	31
4.5.1 Surface complexation modelling	32

4.5.2	Geochemical modelling of soils	34
<b>5</b>	<b>Results and discussion</b>	<b>35</b>
5.1	Phosphate effects on copper(II), lead(II) and cadmium(II) sorption to ferrihydrite	35
5.1.1	Single sorbate systems	35
5.1.2	Phosphate effects	37
5.1.3	Structures of surface complexes: EXAFS spectroscopy	37
5.1.4	Surface complexation modelling	39
5.2	Arsenate sorption to ferrihydrite and poorly crystalline aluminium hydroxide	41
5.2.1	Arsenate and phosphate adsorption on pure sorbents	41
5.2.2	Arsenate and phosphate adsorption on mixed sorbents	41
5.3	Zero-valent iron stabilisation of copper and arsenic	43
5.3.1	Leachable copper and arsenic	43
5.3.2	Immobilising mechanisms	44
5.3.3	Scenario modelling	45
5.4	Phosphate effects on sorption of lead(II), copper(II) and cadmium(II) to podzolised soils	46
5.4.1	Soil properties	46
5.4.2	Metal sorption	46
5.4.3	Cadmium coordination in two B-horizons	50
	<b>Conclusions</b>	<b>53</b>
	<b>Implications and future research</b>	<b>55</b>
	<b>References</b>	<b>57</b>
	<b>Acknowledgements</b>	<b>65</b>

## List of Publications

This thesis is based on the work contained in the following papers, referred to by Roman numerals in the text:

- I Tiberg, C., Sjöstedt, C., Persson, I., Gustafsson, J.P. (2013). Phosphate effects on copper(II) and lead(II) sorption to ferrihydrite. *Geochimica et Cosmochimica Acta* 120, 140-157. doi: 10.1016/j.gca.2013.06.012.
- II Tiberg, C., Gustafsson, J.P. (2016). Phosphate effects on cadmium(II) sorption to ferrihydrite. *Journal of Colloid and Interface Science* 47, 103-111. doi: 10.1016/j.jcis.2016.03.016
- III Tiberg, C., Kumpiene, J., Gustafsson, J.P., Marsz, A., Persson, I., Mench, M., Kleja D.B. (2016). Immobilization of As and Cu in two contaminated soils with zero-valent iron – Long term performance and mechanisms. *Applied Geochemistry* 67, 144-152. doi: 10.1016/j.apgeochem.2016.02.009
- IV Tiberg, C., Sjöstedt, C., Eriksson, A.K., Gustafsson, J.P. Phosphate competition with arsenate on poorly crystalline iron and aluminium (hydr)oxides. Manuscript.

Papers I-III are reproduced with the permission of the publishers.

The contribution of Charlotta Tiberg to the papers included in this thesis was as follows:

- I Participated in planning. Performed batch experiments with copper(II) and assisted in collection of XAS spectra. Performed EXAFS data analysis and surface complexation modelling together with the co-authors. Wrote the manuscript together with the co-authors.
- II Participated in planning. Performed batch experiments. Collected XAS spectra with assistance from the co-author. Performed EXAFS data analysis including WT. Performed surface complexation modelling with advice from the co-author. Wrote the manuscript with assistance from the co-author.
- III Planned the study together with the co-authors. Performed parts of the laboratory work. Collected XAS spectra with assistance. Performed EXAFS data analysis and geochemical modelling with assistance from the co-authors. Wrote the manuscript with assistance from the co-authors.
- IV Planned the study. Performed the laboratory work and EXAFS measurements. Took part in XAS data analysis. Performed surface complexation modelling. Performed the writing together with the co-authors.

## Abbreviations

Alhox	Poorly crystalline aluminium hydroxide
ATR-FTIR	Attenuated total reflectance Fourier transform infrared
CD	Charge distribution
CD-MUSIC	Charge distribution multisite complexation
CN	Coordination number
DOC	Dissolved organic carbon
DOM	Dissolved organic matter
EXAFS	Extended X-ray absorption fine structure
Fh	Ferrihydrite
FT	Fourier transform
HSAB	Hard and soft acids and bases
ICP-MS	Inductively coupled plasma-mass spectrometry
ICP-OES	Inductively coupled plasma-emission spectrometry
ICP-SFMS	Inductively coupled plasma-sector field mass spectrometry
LCF	Linear combination fitting
PZC	Point of zero charge
SCM	Surface complexation model
SHM	Stockholm Humic Model
SOM	Solid organic matter
WT	Wavelet transform
XANES	X-ray absorption near-edge structure
XAS	X-ray absorption spectroscopy
XRD	X-ray diffraction
ZVI	Zero-valent iron



# 1 Introduction

All over the world, elements and compounds occur in concentrations that can be harmful to organisms. This may be due to ‘natural’ processes, but the cause is often enrichment or manufacture of toxic substances by humans. Harmful substances in soil and water are usually called contaminants, regardless of whether they are a result of human influence or not.

Soil contamination has been identified as an important issue in the European Union soil thematic strategy (COM(2006) 231). Based on reporting from 27 European countries, 1,170,000 potentially contaminated sites have been identified, with the most frequent contaminants being heavy metals and mineral oils (van Liedekerke *et al.*, 2014). Thus soil contamination is an important environmental challenge of our time.

In order to predict the behaviour of contaminants in the environment, it is crucial to understand the mechanisms behind their mobilisation/immobilisation on a molecular scale. If the mechanisms are known, it is possible to predict to what extent contaminants are transported and available for uptake in plants, animals, humans *etc.*, even under changing environmental conditions. Consequently, knowledge of mobilisation/immobilisation mechanisms is a key for risk assessments and for development of new methods for remediation of soils, waters and other contaminated materials.

One challenge when working on a molecular scale is to transfer the knowledge to a macroscopic scale. As environmental systems are usually complex, much knowledge has to be compiled to understand a system and to make predictions on a macroscopic level. A powerful tool for assembling knowledge about geochemical processes is to describe them in a thermodynamic/mechanistic geochemical model. If the dominant processes in a matrix are described sufficiently well, the model acts as a bridge between the knowledge about molecular processes and observations or predictions on a macroscopic level. The model can then be used to simulate *e.g.* how the

concentration of contaminants in soil water is affected by changes in pH or the extent of contaminant sorption to a reactive barrier/filter or soil amendment.

This thesis focuses on metal binding on the surface of iron (hydr)oxides (also known as iron oxide-hydroxides or iron oxyhydroxides), especially ferrihydrite, which has a large influence on the mobility of many elements in soil (Jambor & Dutrizac, 1998). While the sorption of elements to isolated iron (hydr)oxides is often quite well known, the interactions in more complex mixtures of solid phases are less well understood although they are important for the distribution of elements in soils and other matrices, such as reactive filters. In this thesis the focus is on interactions with phosphate, which is omnipresent in soils and waters. Phosphorus is essential for living organisms and often added to soils improve their fertility.

## 2 Aim

### 2.1 Overall aim

The overall aim of this thesis was to improve the understanding of lead(II), copper(II), cadmium(II) and arsenate binding to iron (hydr)oxides. The focus was on how phosphate affects the sorption on ferrihydrite and in soils where ferrihydrite is an important component.

### 2.2 Specific objectives

The specific objectives of the work were as follows:

To investigate phosphate effects on the sorption of lead(II), copper(II) and cadmium(II) to ferrihydrite, to identify the interactions with phosphate on a molecular scale and to improve a surface complexation model by accounting for the interactions (Papers I and II).

To investigate the long-term effect of zero-valent iron (ZVI) addition on dissolved arsenic and copper, to identify the mechanism(s) responsible for immobilisation and to predict the concentrations of dissolved copper and arsenic in different scenarios using a geochemical model (Paper III).

To investigate how addition of phosphate affects the sorption of arsenate to ferrihydrite, poorly crystalline aluminium hydroxide and mixtures of these sorbents (Paper IV).

To investigate how phosphate affects the sorption of lead(II), copper(II) and cadmium(II) to B- and C-horizons of podzolised forest soils (unpublished).



## 3 Background

### 3.1 Iron and aluminium (hydr)oxides

Iron and aluminium (hydr)oxide surfaces adsorb metal ions, arsenate and phosphate. Their surfaces are generally amphoteric, i.e. the surface charge is pH-dependent. Sorption of anions is favoured at low pH, while sorption of cations is favoured at high pH. At the point of zero charge (PZC), the surface has a zero net charge. Near the PZC (which is different for different (hydr)oxides), both anions and cations are sorbed. The PZC of iron (hydr)oxides lies between 6 and 10 (Cornell & Schwertmann, 2003), while aluminium hydroxides often have somewhat higher PZC, usually between 8.1 and 10 (Goldberg *et al.*, 1996). It has been shown that both iron and aluminium (hydr)oxides adsorb many metals and oxyanions strongly by inner-sphere surface complexation (Peacock & Sherman, 2004; Sherman & Randall, 2003; Arai *et al.*, 2001; Spadini *et al.*, 1994).

Another common feature of iron and aluminium (hydr)oxides is that less crystalline (hydr)oxides have a larger reactive surface area and therefore adsorb greater amounts of ions than more crystalline (hydr)oxides. The surface area of ferrihydrite and poorly crystalline aluminium hydroxide has been estimated to as large as  $>600 \text{ m}^2 \text{ g}^{-1}$  (Goldberg, 2002; Davis & Leckie, 1978). Poorly crystalline (hydr)oxides crystallise over time and are more common in young soils such as the soils of northern Europe, which developed after the last glacial period.

Although goethite and haematite usually occur in greater quantities in soil, ferrihydrite has a larger influence on the mobility of ions in many soils because of its exceptionally large sorption capacity (Jambor & Dutrizac, 1998). Aluminium is mostly present in soil as aluminosilicates. The only crystalline aluminium hydroxide that occurs to an appreciable extent in soil is gibbsite. Aluminium also forms poorly crystalline mineral colloids that are highly reactive (Huang *et al.*, 2002). The poorly crystalline aluminosilicates

allophane and imogolite are common in soils and important aluminium phases in for example spodic horizons of Swedish forest soils (Gustafsson *et al.*, 1999).

There are several commercially available products using iron (hydr)oxide-containing adsorbents for cleaning of arsenic-contaminated waters. Since these products are commercial, full details of their technical characteristics are usually not available, but there are *e.g.* products using granular iron oxides or iron nano-particles (Mohan & Pittman Jr, 2007).

### 3.1.1 Ferrihydrite

Ferrihydrite can form when dissolved Fe(II) rapidly oxidises to Fe(III) and precipitates as poorly crystalline nanoparticles. It can also form from rapid hydrolysis of Fe(III). Although considerable attention has been paid to the chemical and physical properties of ferrihydrite, there is still no consensus on its structure (Hiemstra, 2013; Michel *et al.*, 2010; Michel *et al.*, 2007). The PZC of ferrihydrite is around 8. Measurements of the surface area vary considerably; values between 157 and 840 m<sup>2</sup> g<sup>-1</sup> have been reported (Davis & Leckie, 1978). Much of this variation can probably be attributed to underestimates of the surface area by the commonly used BET-N<sub>2</sub> method (Clausen & Fabricius, 2000) and the surface area is probably at the upper part of the reported range (Davis & Leckie, 1978). The large sorption capacity of ferrihydrite, combined with its ability to adsorb both negatively and positively charged ions, is potentially very useful in the cleaning of waste water, groundwater and drinking water.

Each oxygen atom on the surface of ferrihydrite can be bound to either one, two or three iron atoms (*i.e.* singly, doubly or triply coordinated surface oxygens). Singly coordinated oxygens have been identified as most important for metal sorption (Hiemstra & van Riemsdijk, 2009; Spadini *et al.*, 2003).

When ferrihydrite particles age they aggregate and become more ordered in structure. The surface area then decreases. Two types of ferrihydrite, the more disordered '2-line' and the more crystallised '6-line', can be discriminated based on the observed X-ray diffraction (XRD) patterns (Jambor & Dutrizac, 1998). Ferrihydrite is eventually converted into haematite or magnetite. This process may take only days/weeks in a clean ferrihydrite suspension (Das *et al.*, 2011, Colombo & Violante, 1996), but is inhibited by *e.g.* adsorbed ions and interactions with organic matter (Jambor & Dutrizac, 1998). This is why ferrihydrite remains in soil for hundreds of years. Drying decreases the surface area of ferrihydrite (Scheinost *et al.*, 2001). Organic acids (Vermeer *et al.*, 1998) or other minerals (Liu & Hesterberg, 2011) may also decrease the number of sites available for sorption by covering parts of the surface.

Ions initially adsorb quickly to the surface of ferrihydrite and an equilibrium is usually reached within minutes. Despite this, the sorption continues to increase slowly for a long time (months). This has been attributed to slow intraparticle diffusion into micropores (Swedlund *et al.*, 2014; Scheinost *et al.*, 2001), formation of surface precipitates (Anderson & Benjamin, 1990) and slow desorption of other ions such as carbonate (Carabante *et al.*, 2009). Ultimately, adsorbed ions may be incorporated into the mineral matrix as the ferrihydrite ages (Stegemeier *et al.*, 2015; Vu *et al.*, 2013).

### 3.1.2 Mixtures of iron and aluminium (hydr)oxides

Iron and aluminium (hydr)oxides interact with one another through co-precipitation, sequential precipitation and agglomeration (Anderson & Benjamin, 1990). The properties of phases with both sorbents may therefore differ from the properties of the individual minerals.

The properties of co-precipitated iron/aluminium (hydr)oxides and of mixed suspensions of iron and aluminium (hydr)oxides have been shown to differ from those of the pure solids (Liu & Hesterberg, 2011; Violante & Pigna, 2002; Anderson & Benjamin, 1990). The molar proportion of aluminium to iron seems to be important for the properties of a co-precipitated suspension. At low aluminium concentration (<10-30 mol-% Al), the aluminium tends to be dispersed within the ferrihydrite matrix (Johnston & Chrysochoou, 2016; Harvey & Rhue, 2008; Masue *et al.*, 2007). At higher concentrations of aluminium (~20-80% mol-% Al), the aluminium is often enriched at the surface (Liu & Hesterberg, 2011; Harvey & Rhue, 2008; Anderson & Benjamin, 1990). Ferrihydrite probably precipitates first, providing a substrate for aluminium hydroxide formation. The ferrihydrite surface may then be more or less covered by poorly crystalline aluminium hydroxide and some of the surface sites on the ferrihydrite may not be available for sorption. At a high concentration of aluminium (>80 mol-% Al), discrete aluminium hydroxide particles form (Liu & Hesterberg, 2011; Harvey & Rhue, 2008).

In a natural system where other minerals and organic matter are also present, the interactions will be even more complex.

## 3.2 Sorption of lead(II), copper(II) and cadmium(II) to ferrihydrite

### 3.2.1 Sorption in single sorbate systems

The sorption of lead(II), copper(II) and cadmium(II) to ferrihydrite is highly pH-dependent and stronger at higher pH. Within a limited pH range, the sorption of cations usually increases rapidly with increasing pH, creating a

‘sorption edge’ which describes how the sorption changes with pH. Of these three ions, lead(II) is adsorbed most strongly, while the sorption edge is displaced to higher pH for copper(II). Cadmium(II) is adsorbed rather weakly below pH 6 (Dzombak & Morel, 1990). An increasing metal concentration shifts the adsorption edge to higher pH. The adsorbed ions affect the surface charge and at high surface loadings there is also competition for sorption sites.

Lead(II), copper(II) and cadmium(II) have all been shown to adsorb to ferrihydrite by inner-sphere complexation (Scheinost *et al.*, 2001; Spadini *et al.*, 1994), *i.e.* they share ligands with iron atoms on the ferrihydrite surface. Mono- and bidentate inner-sphere coordination to an iron (hydr)oxide surface is depicted schematically in Figure 1a. Spectroscopic studies suggest that lead(II) mainly bind to ferrihydrite by edge-sharing coordination at higher pH (>5), but there are also indications of monodentate or corner-sharing coordination at lower pH (Trivedi *et al.*, 2003; Scheinost *et al.*, 2001). Copper(II) binding to ferrihydrite is dominated by edge-sharing bidentate complexes at low copper concentrations (Scheinost *et al.*, 2001). At high copper concentrations, copper dimers have been found to adsorb as corner-sharing tridentate complexes to goethite (Peacock & Sherman, 2004). The only spectroscopic study on cadmium(II) complexation to ferrihydrite found in this thesis work identifies a mixture of edge- and corner-sharing bidentate coordination (Spadini *et al.*, 2003). Other studies of cadmium(II) sorption to iron (hydr)oxides (goethite, lepidocrocite) show similar results (Parkman *et al.*, 1999; Randall *et al.*, 1999).

It has been suggested that cations often bind more strongly to a minor part of the surface sites (Benjamin & Leckie, 1981). In a surface complexation model (SCM), this can be considered by introducing ‘high-affinity sites’ that comprise a few percent of the surface sites (Gustafsson *et al.*, 2011; Swedlund *et al.*, 2003; Swedlund & Webster, 2001; Dzombak & Morel, 1990). The nature of these high-affinity sites is not clear and their existence has been questioned. Spadini *et al.* (2003) argue that sites with lower and higher affinity for sorption rather comprise about 50% each of the surface sites on ferrihydrite. They based this estimate on analysis of the surface structure and an SCM with one type of site. The SCM was able to fit cadmium(II) sorption up to about 60% surface coverage, which was comparable to the estimated proportion of sites with higher affinity.

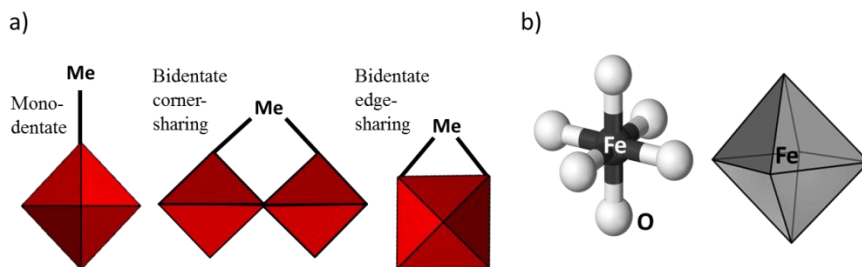


Figure 1. a) Schematic outline of different types of coordination with iron octahedra, monodentate coordination, bidentate corner-sharing coordination and bidentate edge-sharing coordination. b) Two different views of the iron octahedron. The iron, situated in the middle, coordinates to six oxygens.

Ponthieu *et al.* (2006) discuss the differences in complexation on the [110] and [021] planes of ferrihydrite and goethite. They argue that sites with higher affinity are available on the [021] plane because complexes on this plane can coordinate to two ligands on one iron octahedron (edge-sharing coordination) rather than two ligands on two adjacent iron octahedra (corner-sharing coordination) (Figure 1). Spadini *et al.* (2003) also suggested that edge-sharing sites present on the [021] plane have higher affinity.

### 3.2.2 Sorption in ternary systems

Oxyanions can promote the sorption of metals to iron (hydr)oxides (Swedlund *et al.*, 2003; Swedlund & Webster, 2001). There are different explanations for this phenomenon. When anions are added and adsorb to a surface, the surface charge becomes less positive. As a result the sorption of positively charged ions increases. Some authors suggest that this is the sole explanation for increased metal sorption (Collins *et al.*, 1999), but the enhancement caused by electrostatic effects is not always sufficient to explain the whole increase. Another explanation can be a change in metal coordination to the iron (hydr)oxide surface. A modelling study by Venema *et al.* (1997) attributed increased cadmium(II) sorption to goethite in the presence of phosphate to a monodentate Cd-ferrihydrite complex, which was only important in ternary systems. On the other hand, several studies have successfully modelled increased sorption of metals after addition of anions by the introduction of ternary complexes involving the metal, the anion and iron (hydr)oxide surface groups (Nelson *et al.*, 2013; Swedlund *et al.*, 2003; Swedlund & Webster, 2001).

The few existing studies of phosphate effects on lead(II) and cadmium(II) metal sorption to iron (hydr)oxides show that sorption can increase after addition of phosphate (Xie & Giammar, 2008; Wang & Xing, 2002; Venema *et al.*, 1997). On the other hand, Weesner and Bleam (1998) did not observe a clear effect on the sorption of lead(II) to goethite.

The formation of ternary surface complexes with lead(II) and sulphate has been demonstrated in spectroscopic studies (Elzinga *et al.*, 2001; Ostergren *et al.*, 2000). Less spectroscopic information is available for copper(II) sorption in the presence of other anions, but phosphomethylglycine (PMG) has been shown to form ternary complexes with copper(II) on goethite (Sheals *et al.*, 2003). Ternary cadmium(II)-phosphate-haematite surface complexes have been identified by ATR-FTIR (Attenuated total reflectance Fourier transform infrared) spectroscopy (Elzinga & Kretzschmar, 2013). On the other hand, an EXAFS (Extended X-ray absorption fine structure) study by Collins *et al.* (1999) excluded formation of ternary cadmium(II) complexation with phosphate on goethite due to lack of evidence for Cd···P coordination in their EXAFS spectra.

### 3.3 Sorption of arsenate and phosphate to ferrihydrite and poorly crystalline aluminium hydroxide

Arsenate and phosphate ions have a tetrahedral structure and similar chemical properties. It is well known that they compete for sorption sites on iron and aluminium (hydr)oxides (Violante & Pigna, 2002; Manning & Goldberg, 1996). The competitive sorption on mixtures of sorbents has been less well investigated. Such systems are more complex as interactions between the sorbents may affect the sorption.

#### 3.3.1 Sorption in single sorbent systems

Arsenate and phosphate adsorption to ferrihydrite and aluminium hydroxides increases with decreasing pH. However, the effect is attenuated by the protonation of phosphate and arsenate at low pH. As a result, their sorption is less pH dependent than for the metal cations. The pH dependence of the sorption may be slightly different for sorption to iron and aluminium (hydr)oxides as shown by Manning and Goldberg (1996) studying arsenate and phosphate sorption to goethite and gibbsite. The sorption to gibbsite decreased faster with increasing pH (at pH>7) than sorption to goethite for both ions. Arsenate and phosphate exhibit similar sorption to iron (hydr)oxides and a similarly high affinity for ferrihydrite and goethite has been indicated (Gustafsson & Bhattacharya, 2007; Hiemstra & van Riemsdijk, 1999).

A greater difference in affinity between arsenate and phosphate has been observed for aluminium hydroxide surfaces, with phosphate adsorbing more strongly to aluminium hydroxides than arsenate (Violante & Pigna, 2002).

Violante and Pigna (2002) found that iron (hydr)oxide and iron-rich soils were more effective in retaining arsenate than aluminium hydroxides and aluminium-rich soils, while the opposite was true for phosphate. Martin *et al.* (2014) explained a stronger association of arsenate with iron and of phosphate with aluminium by the HSAB (hard and soft acids and bases; Pearson, 1963) theory. Iron is a softer Lewis acid than aluminium. Arsenate, being a softer base than phosphate, should therefore prefer iron and phosphate aluminium. Despite this, ferrihydrite and aluminium hydroxide adsorbed similar amounts of arsenate per surface area due to a higher surface area of the aluminium hydroxide (Martin *et al.*, 2014). Higher arsenate sorption capacity and surface area of poorly crystalline aluminium hydroxide than ferrihydrite was also found by Garcia-Sanchez *et al.* (2002).

The structure of arsenate surface complexes on iron (hydr)oxides has been debated. Several studies used X-ray absorption spectroscopy (XAS) to determine the structure found an As...Fe distance of about 3.3 Å (Loring *et al.*, 2009; Sherman and Randell, 2003; Manceau, 1995; Waychunas *et al.*, 1993). Most studies assign this distance to a bidentate corner-sharing arsenate surface complex (Sherman and Randell, 2003; Manceau, 1995; Waychunas *et al.*, 1993) but Loring *et al.*, (2009) attributed this distance to formation of a monodentate complex on the surface of goethite. Edge-sharing bidentate complexes (As...Fe about 2.7 Å) and a monodentate complex with a longer As...Fe distance (3.6 Å) have also been discussed in the mentioned studies. Inner-sphere bidentate complexes have also been suggested to dominate arsenate sorption to poorly crystalline aluminium hydroxide (Xiao *et al.*, 2015; Arai *et al.*, 2005; Arai *et al.*, 2001).

The structure of phosphate surface complexes has been investigated by Fourier transform infrared spectroscopy (FTIR). Also for phosphate formation of bidentate complexes on the surface of iron (hydr)oxides has been suggested (Arai & Sparks, 2001; Tejedor-Tejedor & Anderson 1990) with possible contribution of monodentate complexes or monodentate complexes that are also coordinated to a second surface group via hydrogen bonding. Persson *et al.* (1996) on the other hand concluded that monodentate complexes dominate phosphate sorption to goethite. Structural investigations of phosphate species sorption to aluminium hydroxide are not conclusive but discuss both monodentate and bidentate complexes (Del Nero *et al.*, 2010; Guan *et al.*, 2005).

The results from spectroscopic studies provide valuable information that can be used to constrain surface complexation models, for example the CD-

MUSIC model (Hiemstra & van Riemsdijk, 1996). Arsenate sorption to ferrihydrite has been simulated with the CD-MUSIC model by Antelo *et al.* (2015) and Gustafsson & Bhattacharya (2007). Two bidentate surface complexes,  $\equiv\text{Fe}_2\text{O}_2\text{AsO}_2^{2-}$  and  $\equiv\text{Fe}_2\text{O}_2\text{AsOOH}$ , were used and dominated sorption at slightly acidic to neutral pH. The presence of additional monodentate species at high or low pH was also discussed (Antelo *et al.*, 2015; Gustafsson & Bhattacharya, 2007). The surface complexation of phosphate to ferrihydrite is analogous to that of arsenate and can be simulated using the corresponding phosphate-containing surface complexes (Antelo *et al.*, 2015; (Antelo *et al.*, 2010; Sjöstedt *et al.*, 2009). Surface complexation modelling of arsenate and phosphate adsorption to poorly crystalline aluminium hydroxides has been limited to date.

### 3.3.2 Sorption to mixed sorbents

As mentioned, it has been found that mixed sorbents may have sorption properties that are different from that which would be expected from simply mixing the sorption properties of the pure end-member phases.

For example, more phosphate and arsenate was adsorbed to co-precipitated iron/aluminium (hydr)oxides (containing 50% Al and less, pH 8) in a study by Violante and Pigna (2002). Direct measurements of arsenate distribution between iron and aluminium in mixtures are scarce, but Suresh Kumar *et al.* (2016) evaluated sorption to co-precipitated iron/aluminium (hydr)oxides by EXAFS spectroscopy. Arsenate sorption could not be attributed to one particular metal hydroxide while arsenite was concluded to adsorb to surface groups on iron (hydr)oxides.

Liu and Hesterberg (2011) showed that phosphate sorption to iron/aluminium co-precipitates was similar to sorption to pure ferrihydrite at low aluminium to iron ratios (< 50% Al), but higher at 75% Al (pH 6). By P K-edge XANES spectroscopy they demonstrated that association with aluminium dominates the phosphate binding when aluminium is present and explained this by enrichment of aluminium at particle surfaces. Harvey and Rhue (2008) showed that more phosphate adsorbed to iron/aluminium co-precipitates containing a high proportion of aluminium.

### 3.4 Partitioning of elements in soil

Soils are usually complex mixtures of minerals and organic matter. Metal contaminants have different properties and are partitioned differently between the soil constituents. One of the reasons why the partitioning is so important is that the total content of a contaminant usually does not relate directly to the risk that it poses. Rather, it is the contaminants that may be transported in the soil and/or are available for uptake by organisms that constitute a risk. This fraction may change with chemical conditions and over time, and therefore understanding of the processes involved is crucial in long-term risk assessments. Important soil compartments for heavy metals and arsenic in soils are schematically summarised in Figure 2.

The composition of the soil solution affects the partitioning of elements. The redox conditions and pH of the soil solution govern the speciation of contaminants to a great extent, as they affect both the speciation in solution and the properties of the solid soil constituents. One example is that although metal cations bind more strongly to iron (hydr)oxides and solid organic matter (SOM) at high pH, their concentration in the soil solution often increases at high pH due to complexation with dissolved organic matter (DOM).

It is well known that lead(II), copper(II) and cadmium(II) all interact strongly with organic matter. Therefore, in addition to the iron and aluminium (hydr)oxides discussed in previous sections, organic matter has to be considered when working with soils. Clay minerals, precipitation of contaminants and weathering of primary minerals were assumed to be of less

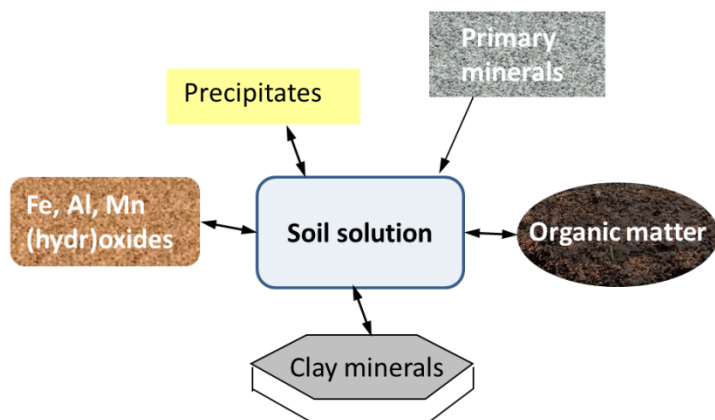


Figure 2. Schematic representation of soil constituents that may affect the concentration of ions in the soil solution.

importance for the systems studied in this thesis. The negatively charged surface of soil organic matter (increasing with pH) mainly attracts cations. Lead(II), copper(II) and cadmium(II) form strong inner-sphere complexes with groups on organic matter. They may also bind by weaker electrostatic interactions (Gustafsson & van Schaik, 2003).

In Figure 2 the solid soil phases are depicted as discrete units. In reality, soil (hydr)oxides and organic matter interact and are commonly present as co-precipitates or assemblages. For example, co-precipitation of iron and aluminium with organic acids is an important process in formation of spodic B-horizons.

#### 3.4.1 Using iron (hydr)oxides for immobilisation of metals and arsenic in soils

Addition of metal (hydr)oxides (or their precursors) has been successfully used for chemical stabilisation of metals and arsenic contaminants in soils in laboratory and pilot-scale field studies (Komarek *et al.*, 2013; Cundy *et al.*, 2008; Kumpiene *et al.*, 2008). One potentially effective immobilising agent is zero-valent iron (ZVI) in the form of iron grit (Kumpiene *et al.*, 2006). In soils, ZVI is rapidly transformed into reactive iron (hydr)oxides (*e.g.* ferrihydrite) with a high surface area and sorption capacity (Komarek *et al.*, 2013), and these can strongly sorb both cations and anions. Furthermore, elements can be co-precipitated with newly formed iron (hydr)oxides (Komarek *et al.*, 2013). Critical factors that affect the immobilisation capacity of oxidised ZVI in soil include pH and redox conditions, the volume of infiltrating water and microbial activity (Kumpiene *et al.*, 2007), as well as the rate of crystallisation of the iron (hydr)oxides formed (Cundy *et al.*, 2008).

The effect of ZVI addition on contaminant mobility has been investigated for a number of elements, including chromium, copper, arsenic and zinc (*e.g.* (Kumpiene *et al.*, 2007; Kumpiene *et al.*, 2006). However, the studies conducted so far have investigated immobilisation in a short-term perspective (months to a few years). For this technique to be recommended as a long-term solution, questions about the long-term performance (several years) remain to be answered. In particular, detailed knowledge about the immobilising mechanisms involved and how they might change over time is needed. Reviews of chemical stabilisation of soils highlight the need for long-term field studies (Komarek *et al.*, 2013; Cundy *et al.*, 2008; Kumpiene *et al.*, 2008).

## 4 Materials and methods

### 4.1 Overview of the experimental work

The focus of this thesis was on metal interactions with ferrihydrite, but experiments were also conducted with soils and poorly crystalline aluminium hydroxide. The minerals and soils used are listed in Table 1.

Batch experiments were conducted to investigate the sorption of metals and arsenic. Molecular-scale binding mechanisms were identified by X-ray absorption (XAS) spectroscopy. Geochemical models able to simulate the results from the batch experiments were then developed based on the XAS results and knowledge about the mineral or soil.

Table 1. *Minerals and soils used in the work described in this thesis*

Ferrihydrite, 2-line	Synthesised in the laboratory according to the procedure of Schwertmann & Cornell (2000). Briefly, a solution containing 36 mmol L <sup>-1</sup> Fe(NO <sub>3</sub> ) <sub>3</sub> and 12 mmol L <sup>-1</sup> NaNO <sub>3</sub> was brought to pH 8.0 by addition of NaOH and aged for 16 h. The suspension was back-titrated to pH 4.6 before use to avoid CO <sub>2</sub> in the solution.
Poorly crystalline aluminium (hydr)oxide	Prepared as ferrihydrite except that Fe(NO <sub>3</sub> ) <sub>3</sub> was replaced by Al(NO <sub>3</sub> ) <sub>3</sub> and the suspension was titrated to pH 7.0 before ageing and back-titrated to pH 5.0 after ageing.
Cu-contaminated soil	Soil from a former wood preservation site in France. Untreated soil (CuUNT) and soil stabilised with 2% ZVI (CuZVI) in 2006. Samples are from subsite P7 (Bes & Mench, 2008), sampled 2012.
As-contaminated soil	Agricultural soil near a former arsenic refinery in Belgium. Untreated soil (AsUNT) and soil stabilised with 1% ZVI (AsZVI) in 1997 (Mench <i>et al.</i> , 2006), sampled 2012.
B- and C-horizons of Swedish forest soils	Coniferous forests soils with, or developing, spodic horizons. Sampled by C. Tiberg and J.P. Gustafsson, May-August 2012.

## 4.2 Characterisation of minerals and soils

Characterisation by XRD confirmed that the expected minerals, 2-line ferrihydrite and poorly crystalline aluminium hydroxide were produced in the mineral synthesis methods applied (Figure 1 in Paper IV).

Characterisation of the contaminated soils focused on parameters required for the geochemical modelling. The ‘geochemically active concentrations’ of metal and major cations participating in equilibrium reactions were estimated by extraction with 0.1 M HNO<sub>3</sub> (16 h) (Gustafsson & Kleja, 2005). The content of poorly crystalline iron and aluminium (hydr)oxides and of geochemically active arsenate was estimated by extraction with oxalate/oxalic acid buffer at pH 3.0 (van Reeuwijk, 1995). The ‘pseudo-total’ content of contaminants and iron in soil was determined after digestion with HNO<sub>3</sub> and H<sub>2</sub>O<sub>2</sub> or melting with LiBO<sub>2</sub>. The organic carbon content and pH were also determined. More details on the characterisation of the contaminated soils are available in Paper III.

For the forest soils, oxalate/oxalic acid and pyrophosphate-extractable iron and aluminium were determined, as well as the pH and organic carbon content.

## 4.3 Batch experiments

The partitioning of elements between liquid and solid phases was determined in batch experiments, either by adding metals to mineral or soil suspension or by studying desorption of metals already present in soil samples. All batch experiments included in the thesis are summarised in Table 2.

Elemental analysis of extracts from batch experiments and extractions was performed using inductively coupled plasma-mass spectrometry (ICP-MS), inductively coupled plasma-sector field mass spectrometry (ICP-SFMS) or inductively coupled plasma-emission spectrometry (ICP-OES). Phosphate was measured colorimetrically (using a Seal Analytical AA3 Autoanalyzer) and DOC content was determined with a Shimadzu TOC 5000 analyser.

### 4.3.1 Batch experiments with ferrihydrite and aluminium hydroxide

Series of batches were prepared to study sorption of lead(II), copper(II) and cadmium(II) to ferrihydrite in the presence and absence of phosphate (Papers I and II). The pH within each series was adjusted with HNO<sub>3</sub> or NaOH to a range of pH values covering the adsorption edge (Table 2). Two additional series where phosphate was replaced with arsenate were prepared in the cadmium study (Paper II). The purpose was to verify that arsenate affected the sorption in the same way as phosphate. If so, arsenate could be used as an

analogue for phosphate in some synchrotron light experiments (see section 4.4.2).

For Paper IV, series of batches were prepared to study arsenate sorption to poorly crystalline aluminium hydroxide and ferrihydrite in competition with phosphate. The series had different Al/Fe ratios and within each series a range of phosphate concentrations (between 0 and 200  $\mu\text{mol L}^{-1}$ ) were added (Table 2). The pH was adjusted to 6.5 before equilibration and again after 1 h of equilibration time in all samples.

Table 2. Summary of batch experiments and XAS measurements presented in this thesis

Metal	Matrix	pH	Batch experiments, series	XAS	Paper
Cu(II) or Pb(II)	Ferrihydrite	3-7	a) 3 mmol L <sup>-1</sup> Fe, 0.3 $\mu\text{mol L}^{-1}$ Cu(II) or Pb(II)		I
			b) 3 mmol L <sup>-1</sup> Fe, 3 $\mu\text{mol L}^{-1}$ Cu(II) or Pb(II)		
			c) 3 mmol L <sup>-1</sup> Fe, 30 $\mu\text{mol L}^{-1}$ Cu(II) or Pb(II)	Cu/Pb	
			d) 0.3 mmol L <sup>-1</sup> Fe, 30 $\mu\text{mol L}^{-1}$ Cu(II) or Pb(II)	Cu/Pb	
<i>All series also with phosphate: 600 <math>\mu\text{mol L}^{-1}</math> to series a, b and c, 60 <math>\mu\text{mol L}^{-1}</math> to series d.</i>					
Cd(II)	Ferrihydrite	4-8	a) 3 mmol L <sup>-1</sup> Fe, 0.3 $\mu\text{mol L}^{-1}$ Cd(II) or Pb(II)		II
			b) 3 mmol L <sup>-1</sup> Fe, 3 $\mu\text{mol L}^{-1}$ Cd(II) or Pb(II)		
			c) 3 mmol L <sup>-1</sup> Fe, 30 $\mu\text{mol L}^{-1}$ Cd(II) or Pb(II)	Cd	
			d) 0.3 mmol L <sup>-1</sup> Fe, 30 $\mu\text{mol L}^{-1}$ Cd(II) or Pb(II)	Cd+As	
<i>All series also with phosphate, series c and d in addition with arsenate: 600 <math>\mu\text{mol L}^{-1}</math> to series a, b and c, 60 <math>\mu\text{mol L}^{-1}</math> to series d.</i>					
Cu(II)	Contaminated soil	4-9	CuUNT: Untreated Cu-contaminated soil	Cu	III
			CuZVI: Stabilised Cu-contaminated soil	Cu	
As(V)	Contaminated soil	4-8	AsUNT: Untreated As-contaminated soil	As	III
			AsZVI: Stabilised As-contaminated soil	As	
As(V)	Ferrihydrite, aluminium hydroxide	~6.5	<i>All series: 58 <math>\mu\text{mol L}^{-1}</math> As + 0, 50, 100 or 200 <math>\mu\text{mol L}^{-1}</math> P added.</i>		IV
			<i>In addition: Sample with only 100 <math>\mu\text{mol L}^{-1}</math> P to 1 mmol L<sup>-1</sup> Al or Fe.</i>		
			1 mmol L <sup>-1</sup> Al	P	
			0.25 mmol L <sup>-1</sup> Fe + 0.75 mmol L <sup>-1</sup> Al	As+P	
			0.5 mmol L <sup>-1</sup> Fe + 0.5 mmol L <sup>-1</sup> Al	As	
			0.75 mmol L <sup>-1</sup> Fe + 0.25 mmol L <sup>-1</sup> Al	As+P	
			1 mmol L <sup>-1</sup> Fe	As	
	As+P				
Cu(II) Pb(II) Cd(II)	Forest soils, B- and C-horizons	4-8	Added concentrations of metals and phosphorus depending on sorption properties and phosphorus content of the soil <sup>a</sup> (Table 3).	Cd to B-horizon	<sup>b</sup>

<sup>a</sup> Cu(II), Pb(II) and Cd(II) added to represent moderately contaminated soils and phosphate added to comply with median concentration in Swedish groundwater, see section 4.3.2.

<sup>b</sup> Not published.

#### 4.3.2 Batch experiments with soils

The solubility of copper and arsenic in untreated and ZVI-treated contaminated soils was investigated over a broad pH range (~4-8) (Paper III).

The sorption of metals to forest soils in the absence and presence of phosphate was investigated by adding metals ( $\text{Pb}(\text{NO}_3)_2$ ,  $\text{Cu}(\text{NO}_3)_2$  and  $\text{Cd}(\text{NO}_3)_2$ ) and phosphate to batches with 2 g soil from B- or C-horizons. The batches were 30 mL in total and had a background electrolyte concentration of 0.01 M  $\text{NaNO}_3$ . The amounts of metals added (Table 3) aimed to represent concentrations in soil water of moderately contaminated soils based on the Swedish EPA generic guideline values for contaminated soils (Swedish Environmental Agency, 2002). The amount of phosphate added aimed at a concentration in the supernatant of about  $0.5 \mu\text{mol L}^{-1}$ , which is half the average concentration of phosphorus in Swedish groundwater ( $\text{PO}_4\text{-P} = 30 \mu\text{g L}^{-1}$ ; SGU, 2013). The batches were equilibrated for 6 days at room temperature before pH was measured. Samples for measurement of cadmium and phosphate were filtered before analysis.

In addition, samples for EXAFS measurements at the cadmium K-edge were prepared with Klotten B and Risfallet B. These samples were prepared in same way as the batch series but with  $100 \mu\text{mol L}^{-1}$  cadmium(II) and  $500 \mu\text{mol L}^{-1}$  phosphate or arsenate.

Table 3. Concentrations of metals and phosphate added to samples of Swedish forest soils in experiments.

Soil profile	Soil horizon	Cu(II) and Pb(II) ( $\mu\text{mol L}^{-1}$ )	Cd(II) ( $\mu\text{mol L}^{-1}$ )	Phosphate ( $\mu\text{mol L}^{-1}$ )
Risfallet	B	30	3	250
Risfallet	C	20	2	50
Tärnsjö	B	24	2.4	30
Tärnsjö	C	20	2	50
Klotten	B	30	3	500
Klotten	C	20	2	70
Risbergshöjden	B	30	3	500
Alnö	B	50	5	50
Alnö	C	30	3	40

## 4.4 X-ray absorption spectroscopy

X-ray absorption spectroscopy (XAS) measurements provide first-hand information about the oxidation state and the local binding environment of an element (Kelly *et al.*, 2008). Spectra are collected at synchrotron radiation facilities by irradiating a sample with high-energy X-rays and measuring how they are absorbed by the sample. Different elements absorb the X-rays at different, well-defined energies (Thompson *et al.*, 2009). The sample is scanned with X-rays across an energy range that covers this absorption energy for the element of interest. The technique is usually non-destructive and measurements for other elements can often be made on the same sample. A number of spectra per sample (between 5 and 20) are collected and averaged to increase data quality. Raw data are generally plotted as measured absorption versus incoming energy. The resulting spectrum includes the energy range around the absorption edge, which is the XANES (X-ray absorption near-edge structure) region, and an additional energy range after the edge, which is the EXAFS (Extended X-ray absorption fine structure) region (Figure 3). The absorption edge of an XAS spectrum moves to higher energy with higher oxidation number and the position can thus be used to identify the oxidation state of the measured element. For example, an arsenic K-edge at about 11,875 eV confirms the presence of arsenic(V) (Mähler *et al.*, 2013).

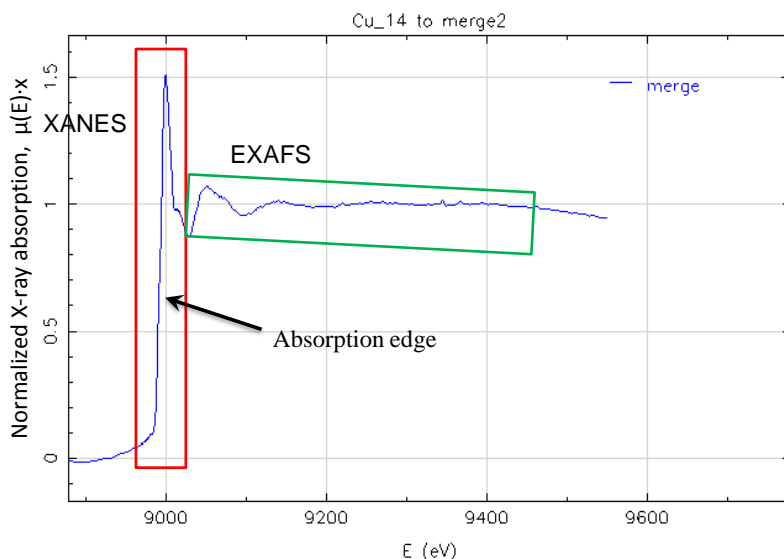


Figure 3. X-ray absorption spectrum collected at the copper K-edge. The XANES region of the spectrum is marked with a red rectangle and the EXAFS region with a green rectangle.

#### 4.4.1 X-ray absorption near edge structure

Phosphorus K-edge XANES spectra were evaluated by linear combination fitting (LCF) to investigate the partitioning of phosphate between iron and aluminium (hydr)oxides (Paper IV). In an LCF, standard spectra of known structures are combined to decide approximately how much of the absorbing element that bind to different constituents in the sample.

#### 4.4.2 Extended x-ray absorption fine structure

An EXAFS spectrum is composed of one or more sine waves, each representing one or more atoms at a certain interatomic distance from the central atom. To extract information from the EXAFS part of a XAS spectrum, a background function (“spline”) is subtracted from the measured spectrum. The Athena software (version 0.8.061 or in the program package Demeter 09.20; Ravel & Newville, 2005) was used for energy calibration, averaging of spectra and background removal.

One common approach to interpreting EXAFS spectra is to develop a structural model of atoms coordinated to the absorber atom that fits the EXAFS spectra. The model gives information about the distance from the absorbing element to neighbouring atoms (Figure 4a). It can also indicate how many they are (the “coordination number”, CN) and what elements they are. The information is compiled to draw conclusions about the surface complexes formed. This approach was used in Papers I, II and III to identify the nature of the lead(II), copper(II), cadmium(II) and arsenate complexes formed. The software Artemis (version 0.8.012; Ravel & Newville, 2005) was used. The model is developed in a trial and error procedure, discarding fits that produce impossible or unlikely parameters (*e.g.* interatomic distances or elements) and deciding on the best fit by comparison of statistical parameters for the fits and visual comparison of measured and modelled spectra. Details of the data treatment are given in the respective paper.

In development of the structural model, Fourier transforms (FT) and Wavelet transforms (WT) of the EXAFS spectra are helpful tools. In FT, the x-axis represents the distance from the central atom and the peaks are signals from backscattering atoms at distinct distances (example in Figure 4b). The WT tool (Papers I-III) helps distinguish between heavy (*i.e.* Fe) and light (*i.e.* O, C) elements. It is useful to also compare the FT and WT plots of measured spectra with FT and WT of model fits in evaluation of model fits.

Heavier elements (*e.g.* As) are easier to detect in analysis of EXAFS spectra than lighter elements (*e.g.* P). Arsenate was therefore added instead of phosphate in some EXAFS samples where the coordination of cadmium(II) was studied. It is also possible to do complementary measurements at the

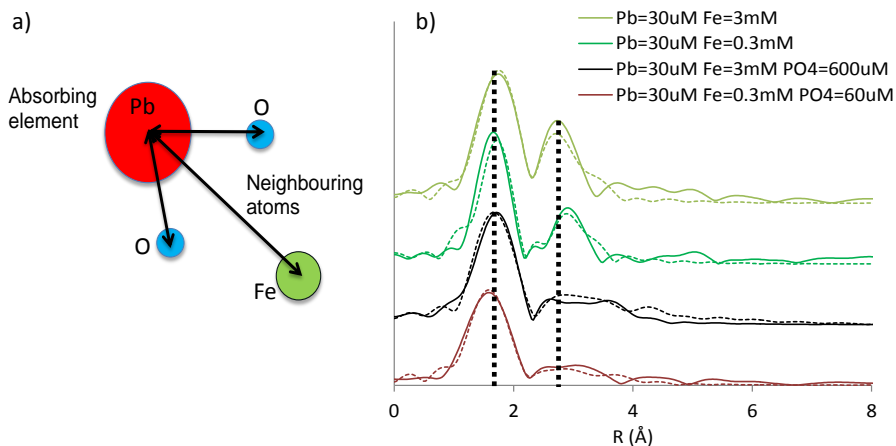


Figure 4. a) Schematic representation of the adsorbing element (red) and neighbouring atoms (blue and green). Arrows denote interatomic distances. b) Fourier transform of a Pb L<sub>3</sub>-edge EXAFS spectrum. The x-axis is not phase-shifted, *i.e.* about 0.5 Å should be added to the distances on the x-axis. The peaks are marked with dashed lines. The first peak is due to coordination with oxygen atoms at ~2.3 Å (illustrated by the blue neighbouring atoms in 4a), while the second peak that is only present in samples 5.2 and 8 is due to iron at ~3.3 Å from the central Pb atom (illustrated by the green atom in 4a).

arsenic K-edge while EXAFS measurements at the phosphorus K-edge are very difficult.

EXAFS spectra can also be evaluated by LCF, as described in section 4.4.1. This technique was used in Paper IV for arsenic K-edge spectra.

#### *Cadmium(II) in the B-horizon of forest soils*

EXAFS spectra for soil samples at the cadmium K-edge were collected at beamline B18, Diamond Light Source, UK, during the same beamtime as the cadmium spectra in Paper II and with the same settings. Data treatment was also performed in the same way. The measurements were made on the solid phase (a wet paste) from the batch experiments. Only the surface of the centrifuged sample was transferred to the aluminium holder. This way coarse material was avoided in the EXAFS measurements.

## 4.5 Geochemical modelling

The most simple geochemical models are empirical models that describe the partitioning between the solid and liquid phase by only one element-specific partitioning coefficient. Empirical models are generally limited to the

conditions under which they were developed (Goldberg, 2007). Thermodynamic models have a more mechanistic approach and model processes in more detail. They can therefore, for example, simulate how changes in pH and ionic strength affect the partitioning of elements and compounds.

Geochemical modelling in this thesis was performed in the chemical equilibrium software package Visual MINTEQ (Gustafsson, 2013). A surface complexation model (SCM) in Visual MINTEQ was used to model sorption of metals to ferrihydrite in detail. For partitioning of metal contaminants between different soil compartments, a number of 'sub-models' were combined into a 'multisurface' model in Visual MINTEQ.

#### 4.5.1 Surface complexation modelling

SCMs describe sorption to surfaces. The charging behaviour of the surface is described in detail and therefore SCMs require a larger number of parameters compared with empirical models. On the other hand, once a SCM is parameterised for a surface, *e.g.* ferrihydrite, it is easy to use and should also be valid for other ferrihydrite surfaces under variable chemical conditions.

Different SCMs differ mainly in how the electrostatic forces at the interface between surface and solution are described. The charge distribution multisite complexation (CD-MUSIC) model (Hiemstra & van Riemsdijk, 1996) that was used for surface complexation modelling in this thesis probably has the most advanced description regarding the electrostatic interactions of the solid-solution interface.

The CD-MUSIC model is a 1-pK model, *i.e.*, the surface protonation is described by one protonation reaction for each type of surface site. Equation 1 shows the reaction for singly coordinated surface oxygens. Different types of surface sites can be distinguished based on the structure of the mineral surface. In line with Hiemstra and van Riemsdijk (2009) and Hiemstra (2013), metals were assumed to react only with singly coordinated oxygens,  $\equiv\text{FeOH}$  surface sites, while protons were assumed to react also with triply coordinated oxygens,  $\equiv\text{Fe}_3\text{O}$  surface sites. The CD-MUSIC model divides the solid-solution interface into three electrostatic planes, the surface plane (the *o*-plane), a 1-plane (also known as the  $\beta$ -plane or inner Helmholtz plane), which is situated in the Stern layer, and the 2-plane (also known as the *d*-plane or outer Helmholtz plane), which coincides with the head-end of the diffuse layer (Figure 5). The capacitance of the surface (C) is described by a combination of the inner and outer layer capacitances,  $C_1$  and  $C_2$ , according to Equation 2.



$$\frac{1}{C} = \frac{1}{C_1} + \frac{1}{C_2} \quad (\text{Equation 2})$$

Furthermore, the charge of inner-sphere complexes is distributed between the surface and the 1-plane, based on the Pauling concept of charge distribution. A fraction  $f$  of the charge of the central cation is attributed to the surface ligand(s) and the remaining part  $(1-f)$  to the ligand(s) in the 1-plane. There are several factors that determine the exact value of  $f$ . Therefore,  $f$  is usually regarded as an adjustable parameter in the CD-MUSIC model. The charge distribution (CD) values,  $\Delta z_0$  and  $\Delta z_1$ , are related to  $f$ . They describe the net change of charge in the surface plane and the 1-plane for a surface complexation reaction (Hiemstra & van Riemsdijk, 1996). In this thesis  $\Delta z_0$  and  $\Delta z_1$  were fitted in the modelling (within reasonable limits) and  $f$  was then calculated (Hiemstra & van Riemsdijk, 1996). A commonly used criterion for constraining  $\Delta z_0$  and  $\Delta z_1$  is that the surface oxygens should not be oversaturated (*i.e.* become positively charged) (Hiemstra & van Riemsdijk, 1996).

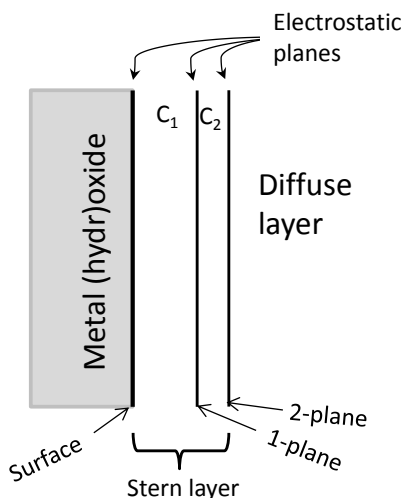


Figure 5. Schematic presentation of the three electrostatic planes in the CD-MUSIC model: the surface plane, the 1-plane and the 2-plane at the head-end of the diffuse layer.  $C_1$  denotes the capacitance between the surface plane and the 1-plane, while  $C_2$  is the capacitance between the 1-plane and the 2-plane.

The CD-MUSIC model was parameterised for ferrihydrite (Paper I) based on the work by Hiemstra and van Riemsdijk (2009) and Hiemstra (2013). So far, no parameterisation of the CD-MUSIC model for poorly crystalline aluminium hydroxide has been published.

Surface complexation constants,  $\Delta Z_0$  and  $\Delta Z_1$ , were optimized in the modelling. For lead(II) and copper(II) interactions with the ferrihydrite surface in the absence and presence of phosphate (Paper I) FITEQL was used (Herbelin & Westall, 1999). Similar systems with cadmium(II) were optimised in Paper II with PEST (Doherty, 2010) which is integrated in Visual MINTEQ.

#### 4.5.2 Geochemical modelling of soils

Optimised models for discrete surfaces can be combined in a ‘multisurface’ model to simulate more complex systems. A multisurface model was designed for the contaminated soils in Paper III to investigate how changes in soil parameters affect the dissolution/desorption of elements. A decisive feature for the performance of such models is to ensure that all important processes are covered by the model.

The multisurface model included speciation of the soil solution, solid and dissolved soil organic matter, iron and aluminium (hydr)oxides and dissolution/precipitation of relevant minerals.

Sorption to iron and aluminium (hydr)oxides was modelled with the ferrihydrite model developed in Papers I and II, *i.e.* both surfaces were assumed to behave as ferrihydrite.

Sorption to solid organic matter (SOM) and dissolved organic matter (DOM) was modelled with the Stockholm Humic model (SHM) with the acid-base parameters of Gustafsson and van Schaik (2003).

The model was not calibrated for the samples investigated. Instead, *a priori* assumptions on the amounts and properties of soil constituents were used (Paper III).

## 5 Results and discussion

### 5.1 Phosphate effects on copper(II), lead(II) and cadmium(II) sorption to ferrihydrite

#### 5.1.1 Single sorbate systems

In line with the amphoteric surface properties of ferrihydrite, adsorption of lead(II), copper(II) and cadmium(II) increased with increasing pH, from about 0% at low pH to 100% at high pH (Figure 6). Lead(II) was strongly adsorbed also at low pH despite a positively charged surface, while copper(II) and cadmium(II) were only adsorbed at higher pH.

Sorption of copper(II) at the three lowest Cu/Fe ratios essentially followed the same adsorption edge (Figure 6c), which indicates that the sorption is independent of the total copper concentration as long as the surface sites of the ferrihydrite surface are far from saturated. By contrast, the adsorption of lead(II) proved to be highly dependent on the lead(II) concentration (Figure 6a), also at low surface coverage, while cadmium(II) showed intermediate behaviour. Similar main features of the sorption patterns have been reported in earlier studies of similar systems (Swedlund *et al.*, 2003; Swedlund & Webster, 2001; Benjamin & Leckie, 1981).

Sorption of phosphate to ferrihydrite (Figure 2 in Paper I) decreased with increasing pH, as expected for surface complex-forming anions (Antelo *et al.*, 2010; Gustafsson & Bhattacharya, 2007).

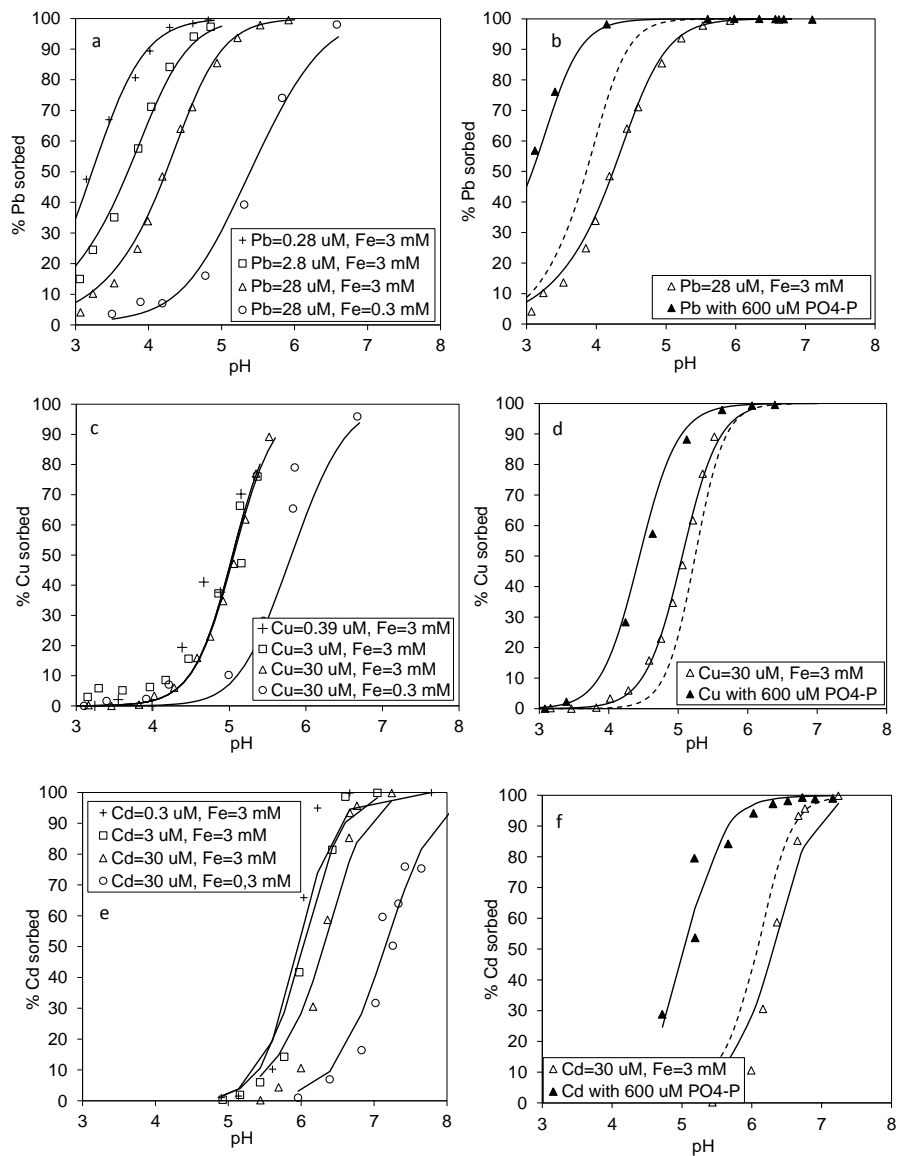


Figure 6. Sorption to ferrihydrite of: a) lead(II) at different Pb/Fe ratios, b) lead(II) in the absence and presence of phosphate, c) copper(II) at different Cu/Fe ratios, d) copper(II) in the absence and presence of phosphate, e) cadmium(II) at different Cd/Fe ratios and f) cadmium(II) in the absence and presence of phosphate. Symbols are data from batch experiments and solid lines are best model fits. Dashed lines are simulation of the systems with phosphate without ternary complexes.

### 5.1.2 Phosphate effects

Phosphate increased the sorption of all metals to ferrihydrite, *i.e.* more of the metal was sorbed at a certain pH when phosphate was added (see examples in Figure 6). The enhancement was greater for lead(II) and cadmium(II) than for copper(II). The effect was smaller at higher surface coverage when the sorption edge was displaced to higher pH and very small for the highest Cu/Fe ratio (Figure 3 in Paper I). A similar effect was observed by Swedlund *et al.* (2003) and Swedlund and Webster (2001) for sorption of metals to ferrihydrite on addition of sulphate.

At the lowest P/Pb and P/Cd ratio ( $60 \mu\text{mol L}^{-1}$  P and  $30 \mu\text{mol L}^{-1}$  Pb or Cd), there was also clear enhancement of phosphate sorption in series with lead(II) or cadmium(II) added compared with a series with only phosphate (Figure 2 in Paper I, Figure 2 in Paper II). In the series with higher phosphate additions ( $600 \mu\text{mol L}^{-1}$ ), the metals had little effect on the phosphate sorption due to the much higher P/Pb and P/Cd ratios.

### 5.1.3 Structures of surface complexes: EXAFS spectroscopy

Based on the interpretation of EXAFS spectra, lead(II), copper(II) and cadmium(II) were concluded to form inner-sphere bidentate complexes on the ferrihydrite surface in single sorbate samples (Papers I and II). Similarly to previous studies (Trivedi *et al.*, 2003; Scheinost *et al.*, 2001), lead(II) and copper(II) edge-sharing complexes with Pb $\cdots$ Fe distances of about 3.4 Å and Cu $\cdots$ Fe distances of about 3.0 Å were identified (Figure 7a). For cadmium(II), two Cd $\cdots$ Fe distances, 3.3 and 3.8 Å, were found and interpreted as evidence of formation of two different bidentate complexes; one edge-sharing and one corner-sharing (Figures 7a and 7b). Similar distances were found by Randall *et al.* (1999) for cadmium(II) sorption to iron (hydr)oxides.

Visible differences in the EXAFS spectra, FT and/or WT between samples indicate different coordination environments around the measured element. Differences between samples with and without phosphate added were especially prominent in the FT of lead(II) EXAFS spectra (see Figure 4), where the second peak in the FT almost disappeared in samples with phosphate. The pattern was similar for copper(II) and cadmium(II); the signal from the Me $\cdots$ Fe distance indicating an edge-sharing complex was weaker in the samples with phosphate. Instead, a longer Me $\cdots$ Fe distance emerged in the phosphate-containing samples (although there was only a weak indication in the case of copper(II)). This longer distance was interpreted as evidence of monodentate or corner-sharing bidentate coordination on the ferrihydrite surface. It could be part of a ternary complex including the ferrihydrite surface,

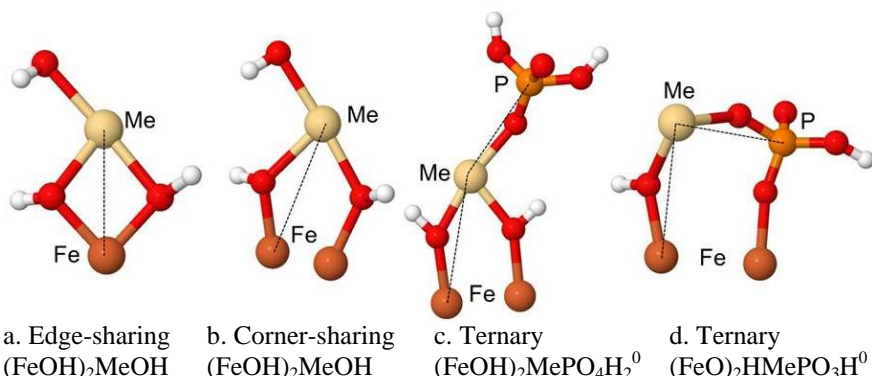


*Figure 7.* Proposed structures for metal surface complexes consistent with EXAFS interpretations and SCM results. Bright red atoms are oxygen, white atoms are hydrogen, Me denotes Pb(II), Cu(II) or Cd(II) atoms. Dashed lines show interatomic distances for the complexes. The complex shown in (b) was only proposed for cadmium(II). In principle, P can be exchanged for As to illustrate arsenic-containing samples.

the metal and the phosphate (Figures 7c and d). In a ternary complex, the metal would also be bound to phosphate. Metal-phosphate distances could only be identified in the samples with cadmium(II) (as well as an Cd···As distance in the corresponding arsenate containing sample). However, the absence of metal-phosphorus distances in lead(II)- and copper(II)-containing samples does not rule out the formation of ternary complexes. Phosphorus is a light element and therefore not easy to detect by EXAFS spectroscopy. Combined with the relatively poor spectral quality of the lead(II) spectra, a Pb···P distance would be difficult to distinguish. Formation of rather few ternary copper complexes at the pH of EXAFS samples (5.85 and 6.58) could be one reason why a Cu···P distance was not identified. The interaction with phosphorus may also be of an outer-sphere nature for some metals, in which case the metal-phosphorus distances would be long, with a wide distance distribution, and therefore impossible to identify.

Earlier spectroscopic studies (XAS and IR spectroscopy) of related systems mostly include complexes formed on goethite. Ternary complexes have been identified, *e.g.* lead-sulphate-goethite complexes (Elzinga et al., 2001; Ostergren et al., 2000) and phosphate-cadmium(II)-goethite complexes (Elzinga & Kretzschmar, 2013).

In summary, the EXAFS measurements of lead(II), copper(II) and cadmium(II) showed that there was a change in metal coordination to the ferrihydrite surface when phosphate was added and that this change could be induced by formation of ternary complexes.

#### 5.1.4 Surface complexation modelling

Surface charging parameters for ferrihydrite in the CD-MUSIC model were determined in Paper I and used in all subsequent ferrihydrite modelling.

Based on the results from EXAFS spectroscopy, the lead(II), copper(II) and cadmium(II) model reactions were defined as bidentate complexes (Table 4). The best modelling results were obtained with the assumptions that the adsorbed copper(II) and cadmium(II) were hydrolysed, whereas lead(II) was not (Table 4). As indicated by the dependence on sorbate concentration, modelling of lead(II) and cadmium(II) sorption was improved by the introduction of site heterogeneity. The surface sites were divided into classes with different affinity and a small proportion of the surface sites was assigned higher affinity, in line with previous modelling of similar systems by Dzombak and Morel (1990) and Swedlund *et al.* (2003). For cadmium(II), two different site affinities, corresponding to 99% and 1% of the surface sites, yielded good fits, but for lead(II) three different affinities, corresponding to 99%, 0.9% and 0.1%, were required (Table 4, see also Figure 6). For copper(II) and cadmium(II) surface complexes the  $\Delta z_0$  and  $\Delta z_1$  were fitted to 0.5 for both the surface plane and the 1-plane. The fraction  $f$  of charge attributed to the surface was then 0.25, which can be considered realistic. The lead surface complex had an unusually large fraction of charge attributed to the surface ( $f = 0.6$ ), which would create slight oversaturation of the surface oxygen ligands. This could be due to a weak interaction with a third surface group not explicitly included in the model, as discussed by Gustafsson *et al.* (2011). Phosphate and arsenate sorption was modelled with the complexes and constants listed in Table 4.

A surface complexation model with only bidentate metal-ferrihydrite complexes was unable to simulate sorption of lead(II), copper(II) and cadmium(II) in the phosphate-containing systems, *i.e.* electrostatic effects alone could not satisfactorily explain the enhanced sorption after phosphate addition (see dashed lines in Figure 6). This was in line with results from EXAFS spectroscopy showing that metal coordination changed upon addition of phosphate. Better agreement with experimental data was obtained by adding a ternary surface complex with the surface reactions and complexation constants given in Table 4. This complex, depicted in Figure 7d, is consistent with interpretation of the EXAFS data. Fitting of the CD values for the ternary complexes yielded  $f = 0.24$ , which would leave the surface oxygens slightly undersaturated. It should be noted that the description in the CD-MUSIC model of the ternary complex depicted in Figure 7c, where the metal is bidentately coordinated to the ferrihydrite surface, would be the same as for 7d.

Site heterogeneity was applied for ternary lead(II) complexes (1% of the sites were assigned higher affinity) but not for copper(II) and cadmium(II).

Table 4. *Surface complexation reactions and optimised constants used in the CD-MUSIC model for metal sorption to ferrihydrite*

Reaction	$(\Delta z_0, \Delta z_1, \Delta z_2)^a$	$\log K^b$
$2\text{FeOH}^{1/2-} + \text{Pb}^{2+} \leftrightarrow (\text{FeOH})_2\text{Pb}^+$	(1.2,0.8,0)	9.58 (99%) 12.25 (0.9%) 14.24 (0.1%)
$2\text{FeOH}^{1/2-} + 2\text{H}^+ + \text{Pb}^{2+} + \text{PO}_4^{3-} \leftrightarrow (\text{FeO})_2\text{HPbPO}_3\text{H}^0 + \text{H}_2\text{O}$	(0.7,0.3,0)	33.64 (99%) 37.20 (1%)
$2\text{FeOH}^{1/2-} + \text{Cu}^{2+} + \text{H}_2\text{O} \leftrightarrow (\text{FeOH})_2\text{CuOH} + \text{H}^+$	(0.5,0.5,0)	0.97
$2\text{FeOH}^{1/2-} + 2\text{H}^+ + \text{Cu}^{2+} + \text{PO}_4^{3-} \leftrightarrow (\text{FeO})_2\text{HCuPO}_3\text{H}^0 + \text{H}_2\text{O}$	(0.7,0.3,0)	31.7
$2\text{FeOH}^{1/2-} + \text{Cd}^{2+} + \text{H}_2\text{O} \leftrightarrow (\text{FeOH})_2\text{CdOH} + \text{H}^+$	(0.5,0.5,0)	-1.42 (99%) 1.31 (1%)
$2\text{FeOH}^{1/2-} + 2\text{H}^+ + \text{Cd}^{2+} + \text{PO}_4^{3-} \leftrightarrow (\text{FeO})_2\text{HCdPO}_3\text{H}^0 + \text{H}_2\text{O}$	(0.7,0.3,0)	30.50 <sup>d</sup>
$2\text{FeOH}^{1/2-} + 2\text{H}^+ + \text{Cd}^{2+} + \text{AsO}_4^{3-} \leftrightarrow (\text{FeO})_2\text{HCdAsO}_3\text{H}^0 + \text{H}_2\text{O}$	(0.7,0.3,0)	30.01 <sup>d</sup>
$2\text{FeOH}^{1/2-} + 2\text{H}^+ + \text{PO}_4^{3-} \leftrightarrow \text{Fe}_2\text{O}_2\text{PO}_2^{2-} + 2\text{H}_2\text{O}$	(0.46,-1.46,0)	27.59
$2\text{FeOH}^{1/2-} + 3\text{H}^+ + \text{PO}_4^{3-} \leftrightarrow \text{Fe}_2\text{O}_2\text{POOH}^- + 2\text{H}_2\text{O}$	(0.63,-0.63,0)	32.89
$\text{FeOH}^{1/2-} + 3\text{H}^+ + \text{PO}_4^{3-} \leftrightarrow \text{FeOPO}_3\text{H}_2^{1/2-} + \text{H}_2\text{O}$	(0.5,-0.5,0)	30.22
$2\text{FeOH}^{1/2-} + 2\text{H}^+ + \text{AsO}_4^{3-} \leftrightarrow \text{Fe}_2\text{O}_2\text{AsO}_2^{2-} + 2\text{H}_2\text{O}$	(0.47,-1.47,0)	27.36
$2\text{FeOH}^{1/2-} + 3\text{H}^+ + \text{AsO}_4^{3-} \leftrightarrow \text{Fe}_2\text{O}_2\text{AsOOH}^- + 2\text{H}_2\text{O}$	(0.58,-0.58,0)	32.42
$\text{FeOH}^{1/2-} + 3\text{H}^+ + \text{AsO}_4^{3-} \leftrightarrow \text{FeOAsO}_3\text{H}_2^{1/2-} + \text{H}_2\text{O}$	(0.5,-0.5,0)	29.5

<sup>a</sup>The change of charge in the surface plane (*o*-plane), 1-plane (*b*-plane) and 2-plane (*d*-plane), respectively.

<sup>b</sup>Two or three numbers indicate binding to sites with different affinity, the percentages of which are within brackets (*cf.* text).

The model with ternary complexes was also able to simulate the effect of lead(II) and cadmium(II) on phosphate sorption at high Me/Fe ratio (Figure 2 in Paper I and Figure 2 in Paper II).

The results from geochemical modelling combined with the EXAFS results strongly indicate that ternary complexes on the ferrihydrite surface can explain the enhanced sorption of lead(II), copper(II) and cadmium(II) in the presence of phosphate.

## 5.2 Arsenate sorption to ferrihydrite and poorly crystalline aluminium hydroxide

### 5.2.1 Arsenate and phosphate adsorption on pure sorbents

Although the ferrihydrite (here denoted Fh) and the poorly crystalline aluminium hydroxide (here denoted Alhox) were prepared by very similar procedures, Alhox was indicated to have a greater sorption capacity than Fh (Figure 2 in Paper IV).

With similar amounts of arsenate and phosphate added per mol iron ( $58 \text{ mmol}_{\text{As}} \text{ mol}_{\text{Fe}}^{-1}$  and  $50 \text{ mmol}_{\text{P}} \text{ mol}_{\text{Fe}}^{-1}$ ), Fh adsorbed  $54 \text{ mmol}_{\text{As}} \text{ mol}_{\text{Fe}}^{-1}$  and  $44 \text{ mmol}_{\text{P}} \text{ mol}_{\text{Fe}}^{-1}$  (*i.e.* 93 and 88%, respectively). In the corresponding Alhox sample, 100% of both anions were adsorbed. When more phosphate was added, it competed strongly with arsenate for sorption sites (Figure 8).

### 5.2.2 Arsenate and phosphate adsorption on mixed sorbents

In samples with both sorbents, arsenate sorption generally increased with a higher proportion of Alhox in the samples (Figure 8a). Arsenate sorption in the pure ferrihydrite system deviated from this pattern; here the sorption was higher than in Alhox-containing samples when  $200 \text{ mmol}_{\text{P}} \text{ mol}_{\text{Fe+Al}}^{-1}$  were added. Sorption of phosphate increased with higher Alhox content (Figure 8b). Even with  $200 \text{ mmol}_{\text{P}} \text{ mol}_{\text{Fe+Al}}^{-1}$  added, most of the phosphate was adsorbed in samples with  $\geq 50\%$  Alhox.

Linear combination fitting of results from XAS spectroscopy revealed that more arsenate and phosphate was adsorbed to Alhox than Fh in samples with both sorbents when only arsenate or phosphate was added (Paper IV, Figure 7). At 50% Alhox content, about 65% of the arsenate was adsorbed to Alhox and the phosphate association with Alhox was even stronger. At 50% Alhox content, 85% of the phosphate was adsorbed to Alhox. This is in line with higher sorption capacity of Alhox, but also indicates higher affinity for sorption of phosphate than arsenate to Alhox.

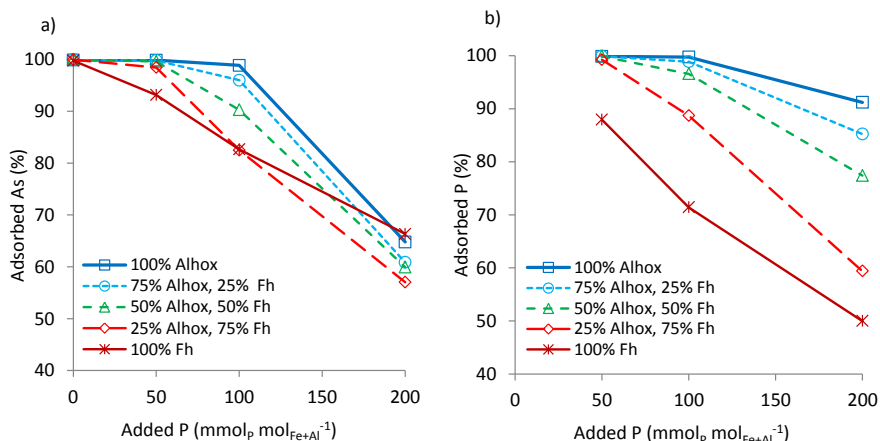


Figure 8. Sorption of arsenate and phosphate on mixed sorbents. 58 mmol<sub>As</sub> mol<sub>Fe+Al</sub><sup>-1</sup> added in all samples: a) percentage of adsorbed arsenate, b) percentage of adsorbed phosphate.

A stronger affinity of phosphate for Alhox should result in stronger competition with arsenate for sorption sites on Alhox than on Fh. In spite of this, a comparison between the LCF results for arsenic EXAFS spectra and the calculated adsorption if arsenate were to be equally distributed between Alhox and Fh (in proportion to their molar concentration in the sample) showed that more arsenate than expected from equal distribution was generally adsorbed to Alhox (Figure 9). A higher surface area of Alhox could be the explanation. An additional reason could be enrichment of aluminium on the surface of Fh particles. This may be relevant if the concentration of aluminium is between 20 and 80% on a molar basis (Liu & Hesterberg, 2011; Harvey & Rhue, 2008; Anderson & Benjamin, 1990).

Two samples deviated from the general pattern in Figure 9a, namely those with the highest content of Alhox and the highest additions of phosphate, in which equal amounts of arsenate were adsorbed to Alhox and Fh. This might be explained by formation of discrete aluminium hydroxide particles at high Al/Fe-ratio (Liu & Hesterberg, 2011; Harvey & Rhue, 2008). That is, if the tendency of aluminium to enrich at and partly cover the ferrihydrite surface decreases when discrete Alhox particles are formed.

Results from LCF analysis of P K-edge XANES for samples with 50% Alhox, 50% Fh revealed that a larger percentage of phosphate was adsorbed to Alhox in all samples (Figure 9b). The percentage adsorbed to Alhox increased with an increasing proportion of arsenate in the samples, *i.e.* arsenate competed more strongly for sorption sites on Fh than Alhox.

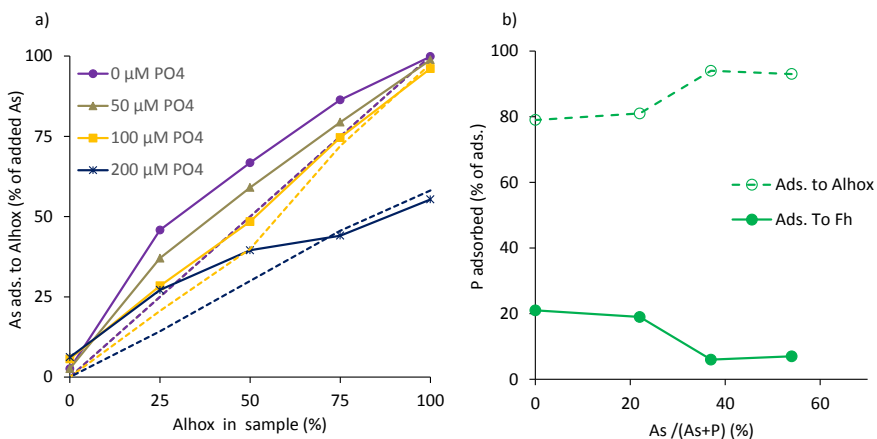


Figure 9. a) Results from LCF of As EXAFS showing the percentage of added arsenate adsorbed to Alhox at different Alhox:Fh ratios and phosphate additions. The dashed lines are percentage of arsenate adsorbed to Alhox (proportional to Alhox content) if arsenate was adsorbed equally to Alhox and Fh (0 and 50 mmol<sub>P</sub> mol<sub>Fe+Al</sub><sup>-1</sup> additions overlay due to 100% sorption of arsenate). b) Results from P K-edge XANES spectroscopy showing percentage of adsorbed phosphate as a function of the proportion of arsenate in the samples.

## 5.3 Zero-valent iron stabilisation of copper and arsenic

### 5.3.1 Leachable copper and arsenic

In general, less copper and arsenic were desorbed from the ZVI-treated soils than the untreated soils. At the original soil pH, the dissolved copper concentration was 70% lower in CuZVI than CuUNT. A higher concentration of soluble copper at low pH in the ZVI-treated soil (Figure 1, Paper III) can be explained by a combination of higher copper concentration and lower SOM concentration in this sample compared with CuUNT. Arsenic was more soluble at high pH. At the original soil pH (about 8), dissolved arsenic was reduced by 50% in AsZVI compared with AsUNT, whereas at pH 5 dissolved arsenic decreased by 95% as a result of ZVI stabilisation.

The multisurface geochemical model accurately predicted the measured concentrations of copper (Figure 1, Paper III), especially bearing in mind that generic parameters and ‘standard’ assumptions were used in the model setup. The dissolved arsenic concentration was generally somewhat underestimated by the model, but the pH dependence was replicated (Figure 10).

### 5.3.2 Immobilising mechanisms

Simulations of copper partitioning in the soil predicted that copper was primarily associated with SOM within the whole pH range in CuUNT, whereas there was a shift towards sorption to iron and aluminium (hydr)oxides in CuZVI, especially at high pH (Figure 2 in Paper III). Arsenic was predicted to bind to iron and aluminium (hydr)oxides in both untreated and ZVI-treated soil.

The predicted immobilisation mechanisms were confirmed by analysis of EXAFS spectra. Copper was primarily bound to organic matter in CuUNT. The Cu···C distance ( $\sim 2.8$  Å) and multiple scattering paths found are in agreement with binding in a copper(II)-chelate ring structure known to be important in soils (Strawn & Baker, 2009; Karlsson *et al.*, 2006). Copper in the ZVI-treated soil was primarily bound to iron as inner-sphere bidentate complexes (Cu···Fe  $\sim 3.0$  Å), the same complex as used for copper sorption to ferrihydrite in the multisurface model based on the findings in Paper I.

Arsenic was present as arsenate in both soil samples, as confirmed by the position of the peak of the arsenic absorption edge at about 11,875 eV. Evaluation of arsenic EXAFS spectra indicated bidentate bonding to both iron and aluminium (hydr)oxide surfaces in AsUNT. In AsZVI binding to iron (hydr)oxide surfaces dominated. Both the As···Fe ( $3.4$  Å) and the As···Al distances ( $3.2$  Å) found were close to the values reported in earlier studies, with an As···Fe distance of  $3.3$ - $3.4$  Å (Sherman & Randall, 2003) and an As···Al distance of  $3.1$ - $3.2$  Å (Xiao *et al.*, 2015; Arai *et al.*, 2001). In the scenario modelling, the sorption to both iron and aluminium (hydr)oxides was simulated by the same bidentate complex. This simplification was supported by the spectroscopic results.

Arsenate sorption to both aluminium and iron (hydr)oxides in AsUNT and mostly to iron (hydr)oxides in AsZVI is consistent with estimates of reactive iron and aluminium (hydr)oxides in the soils. Oxalate extraction indicated one-third iron and two-thirds aluminium (hydr)oxides in AsUNT, while the relationship was the opposite, two-thirds iron and one-third aluminium (hydr)oxides, in AsZVI. It is well known that arsenate adsorbs strongly to both aluminium and iron (hydr)oxides in soil (Hopp *et al.*, 2008; Manning, 2005).

Overall, the interpretation of EXAFS results confirmed the contaminant distribution predicted by the multisurface model: copper was primarily bound to organic matter in CuUNT but to iron (hydr)oxides in CuZVI, while arsenic was associated with aluminium and/or iron (hydr)oxides in both samples.

### 5.3.3 Scenario modelling

The multisurface model was able to predict both the copper and arsenic concentrations in solution and the speciation in the solid phase at the original soil pH (Paper III). It was therefore assumed that the most important retention processes were included and the model was used to investigate key soil factors affecting ZVI stabilisation.

Critical parameters for copper immobilisation include the content of organic matter, the amount of added ZVI and the pH. To investigate the influence of these parameters on copper retention, model calculations were made with different organic matter contents (0.5 or 2% organic carbon) and ZVI additions (1 or 2% ZVI). All other parameters were kept the same in the six simulations. The results showed that stabilisation of copper with ZVI would be most effective in soils with pH above 6 and that the immobilising effect is greater for soils that are relatively low in organic matter (Figure 10).

Experimental data for arsenate were simulated more accurately by decreasing the amount of adsorbing iron/aluminium (hydr)oxide surfaces compared with the amount calculated based on oxalate extraction (Figure 10). This might reflect a tendency for oxalate to overestimate the amount poorly crystalline iron/aluminium (hydr)oxides in this soil. The explanation could also be differences between the properties of the freshly precipitated ferrihydrite

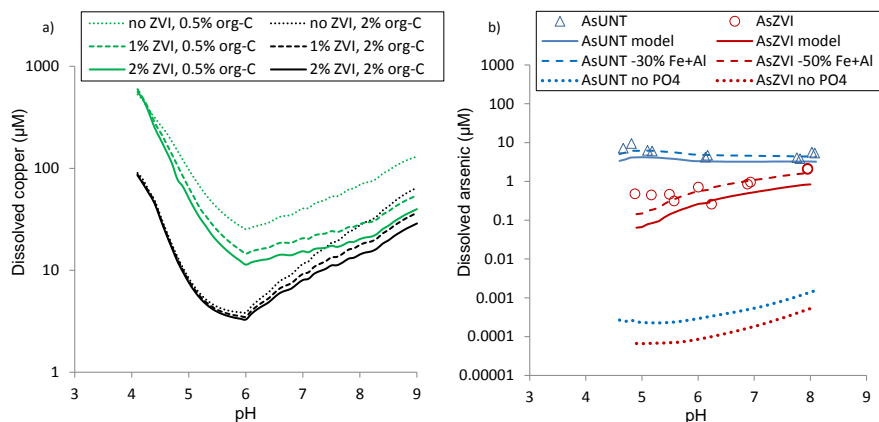


Figure 10. Scenario modelling of ZVI-treated soils. a) Simulation of dissolved copper(II) at different contents of organic matter and different additions of ZVI. Total copper in the simulation was  $100 \mu\text{mol L}^{-1}$ . b) Dissolved arsenic. Symbols are experimental data. Dashed lines are simulations with 30% or 50% less adsorbing iron and aluminium (hydr)oxide surfaces. Dotted lines are simulations without phosphate present. Total arsenic in the simulation  $120 \mu\text{mol L}^{-1}$  for AsUNT and  $140 \mu\text{mol L}^{-1}$  for AsZVI.

that was used to set up the SCM and the properties of the adsorbing iron and aluminium (hydr)oxides in the soil (*e.g.* PZC, surface area). There may also be a need to compensate for ageing processes affecting the sorption capacity of iron and aluminium (hydr)oxides (Stegemeier *et al.*, 2015) and/or blocking of sorption sites by *e.g.* humic substances (Gustafsson, 2006).

Simulations of how phosphate affects the arsenate sorption indicated an increase in arsenate sorption when phosphate was removed from the system. There was about 10-fold more phosphate than arsenate in the supernatant of batch experiments. When phosphate was ignored in the modelling, arsenate concentrations in the supernatant were very much underestimated (Figure 10).

## 5.4 Phosphate effects on sorption of lead(II), copper(II) and cadmium(II) to podzolised soils

### 5.4.1 Soil properties

The sampling sites were chosen to represent varying content of organic matter as well as iron and aluminium (hydr)oxides. All samples had a rather low pH, which is typical for Swedish coniferous forest soils (Table 5). At the original soil pH, dissolved phosphate was only detected in batches with the Tärnsjö and Alnö soils. This does not necessarily mean that these soils have the highest content of phosphorus. Tärnsjö and Alnö had the lowest content of iron and aluminium (hydr)oxides and therefore probably lower sorption capacity than the other soils. As expected, the concentrations of organic carbon and iron/aluminium (hydr)oxides were much lower in the C-horizons than the B-horizons.

### 5.4.2 Metal sorption

The added metal concentrations differed between soil samples (see Table 3). The cadmium(II) addition was 10-fold lower than that of lead(II) and copper(II), reflecting the lower Swedish guideline value for cadmium in contaminated soils.

Table 5. Properties of the forest soils included in the sorption experiments.

Site	Location (Lat, Long)	Hori zon	Soil pH <sup>a</sup>	Org. C (%)	Al <sub>ox</sub> <sup>b</sup>	Fe <sub>ox</sub> <sup>b</sup>	Al <sub>pyr</sub> <sup>b</sup>	Fe <sub>pyr</sub> <sup>b</sup>	Al+Fe <sup>c</sup>	Clay <sup>d</sup> (%)	DOC <sup>e</sup> (mg L <sup>-1</sup> )	PO <sub>4</sub> -P <sup>f</sup> (μg L <sup>-1</sup> )
Risfallet	60.34344°N	Bs	4.24	2.30	265	151	168	86	248	7.0	4.2	<1
	16.21171°E	C	4.36	0.25	85	12	44	7	53	4.2	0.8	<1
Tärnsjö	60.13712°N	B	4.88	0.73	118	45	65	15	98	1.9	1.6	3.3
	16.92145°E	C	5.15	0.04	31	18	9	3	40	0.6	1.6	1.2
Kloten	59.90926°N	Bs	4.73	2.56	647	144	280	70	511	4.0	1.8	<1
	15.25346°E	C	4.55	0.17	75	9	37	6	47	2.2	0.7	<1
Risbergs- höjden	59.71853°N 15.04866°E	Bs	4.39	2.58	534	119	175	29	478	4.0	4.2	<1
Alnö	64.44979°N	B	4.98	0.39	64	93	39	25	118	2.1	1.8	8.5
	17.44006°E	C	5.07	0.09	31	50	12	9	69	2.2	1.1	<1

<sup>a</sup>In 0.01 M CaCl<sub>2</sub>, see Methods section

<sup>b</sup>Subscripts ox and pyr denote oxalate-extractable and pyrophosphate-extractable, respectively

<sup>c</sup>Calculated amount of adsorbing minerals; Fe<sub>ox</sub>+Al<sub>ox</sub>-Al<sub>pyr</sub>

<sup>d</sup>Clay fraction, d<0.002 mm

<sup>e</sup>Measured in batch experiments. Values at pH close to 4.5.

<sup>f</sup>This value refers to PO<sub>4</sub>-P dissolved in 30 ml 0.01 M NaNO<sub>3</sub> at soil pH.

Copper(II) and lead(II) showed similar sorption to the B-horizon soil (Figure 11), with both being 100% removed from solution at about pH 5 and higher. Less copper(II) was adsorbed at low pH in the soils with lower organic matter content, reflecting the high affinity of copper(II) to organic matter. As evidenced in the ferrihydrite experiments (Paper I) copper(II) also has a lower affinity to iron (hydr)oxides at low pH compared with lead(II). Consistent with the high concentrations of DOC in Risfallet B, copper(II) and lead(II) in solution increased at high pH for this soil. A lower percentage of cadmium(II) was retained in the soil B-horizon, despite lower added concentrations (Figure 11c, note the scale on the y-axis). A larger fraction of all metals was found in the soil solution in the C-horizon.

The greatest effect of phosphorus addition could be expected in soils with high levels of iron (hydr)oxides and with a low content of organic matter. Although the B-horizons had much higher content of extractable iron and aluminium (Table 5), iron and aluminium (hydr)oxides are potentially more important in the C-horizons, as these are often very low in organic matter. However, phosphate addition had no obvious effect on the dissolved concentrations of any of the metals in the soils investigated. Dissolved cadmium(II) concentrations were somewhat lower at about pH 5 in Kloten B when phosphate was added, but the difference was very small. Kloten B had the highest content of adsorbing surfaces (calculated as  $Fe_{ox} + Al_{ox} - Al_{pyr}$ ). Ternary cadmium(II)-phosphate-iron complexes are expected to form at this pH, but it could not be confirmed that this caused the observed difference.

The reasons why phosphate did not enhance the sorption in the soil experiments, despite a large influence in the pure ferrihydrite systems, may include the following: i) The metals were mainly bound to organic matter and therefore not much affected by phosphate, ii) the added phosphate did not affect the sorption simply because the added amount was small in comparison with the amount of adsorbed phosphate already present in the soil and iii) the added phosphate was too low in relation to the amount of iron (hydr)oxide surfaces in the soils and therefore had a small influence on the sorption of iron (hydr)oxides. In relation to the third point, it should be noted that the P/Fe ratio expressed as added phosphate in relation to  $Fe_{ox}$  in soils was much lower than the P/Fe ratio in the batch experiments with ferrihydrite. The importance of the first point was supported by spectroscopic measurements at the cadmium K-edge (section 5.4.3).

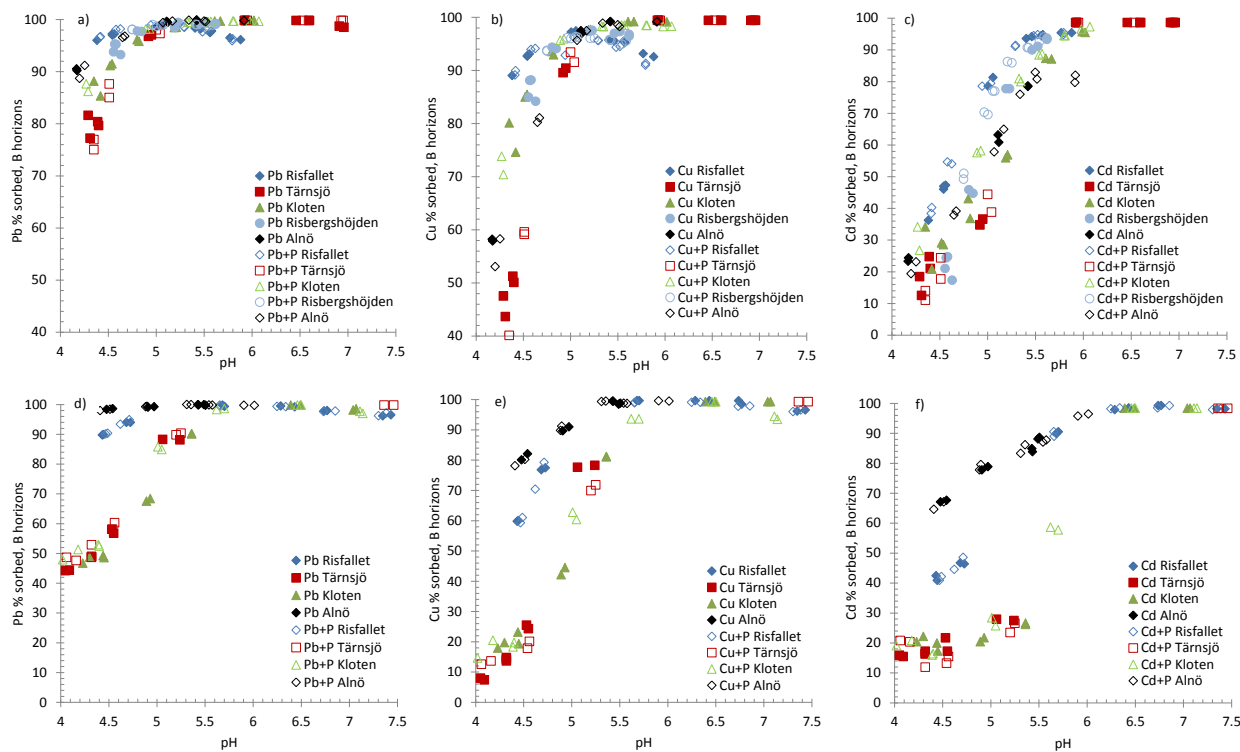


Figure 11. Sorption of lead(II), copper(II) and cadmium(II) to Swedish forest soils with and without addition of phosphate. a) Lead(II) to B-horizon, b) copper(II) to B-horizon, c) cadmium(II) to B-horizon, d) lead(II) to C-horizon, e) copper(II) to C-horizon and f) cadmium(II) to C-horizon.

The fact that the strong enhancement of sorption identified for pure ferrihydrite systems could not be observed in the studied soils does not exclude enhancement of metal sorption by phosphate in other soils. This could still be expected in soils with a higher proportion of iron (hydr)oxides to organic matter, especially if more phosphate is added than in this study. Further evaluation of the results from this study by *e.g.* geochemical modelling could increase the understanding of the retention processes.

#### 5.4.3 Cadmium coordination two B-horizons

EXAFS spectra collected at the cadmium K-edge permitted closer evaluation of cadmium(II) binding mechanisms in the B-horizons of Klotten and Risfallet. The EXAFS spectra for cadmium(II) adsorbed to Klotten B (X2, X6, X7 in Figure 12) and Risfallet B (Y2 and Y7 in Figure 12) were very similar in shape, regardless of whether phosphate or arsenate was added or not. They also resembled the spectrum for cadmium(II) adsorbed to fulvic acid (Cd-FA), indicating that the cadmium(II) was bound in a similar way in all these samples. A spectrum for cadmium(II) adsorbed to ferrihydrite (H7 in Figure 12) had a slightly different shape, for example at k 7-8.

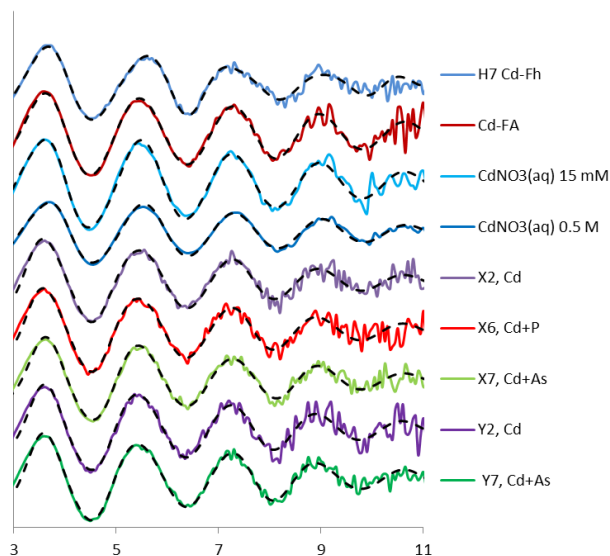


Figure 12. EXAFS spectra of soil samples and standards. Lines are measured spectra, dashed lines are model fits.

Model fits of EXAFS spectra showed that cadmium(II) was coordinated to six oxygens in the first shell of all samples (Table 6). Evaluation of WT of the spectra (not shown) did not suggest any binding to heavy elements (*i.e.* iron) in higher shells. Second shell contributions were modelled with 1.5 carbon atoms between 3.09 and 3.16 Å, the same Cd···C distance as identified by Karlsson *et al.* (2005) for cadmium(II) binding in organic soils.

The sorption of cadmium(II) in the soil samples was evidently dominated by inner-sphere complexes to oxygen-containing groups on organic matter at the ambient pH values. Cadmium(II) has been shown to bind even more strongly to sulphur in thiol groups of soil organic matter (Karlsson *et al.*, 2005), but there was no discernible Cd···S distance in the soil samples or Cd-FA in the present study. Sulphur groups are less abundant than oxygen groups on organic matter: the ratio is about 1:100 in natural organic matter (Karlsson *et al.*, 2005). At the relatively high cadmium(II) concentrations used in this study binding with oxygen groups dominated. This is probably the most common situation in cadmium(II)-contaminated soils.

Table 6. Cadmium(II) K-edge EXAFS of B-horizons and standards. Summary of shell fit results<sup>a</sup>. Parameters in italics were constrained during fitting

Sample <sup>b</sup>	Path	CN	R (Å)	$\sigma^2$ (Å <sup>2</sup> )	$\Delta E$ (eV)	$S_0^2$	R (%)
X2 Kloten	Cd–O	6	2.28 (0.01)	0.010 (0.000)	1.92 (0.81)	<i>0.90</i>	0.48
100 $\mu$ M Cd	Cd···C	<i>1.5</i>	3.13 (0.04)	0.018 (0.005)			
pH 6.12	Cd–O–O <sup>c</sup>	<i>18</i>	4.71 (0.06)	<i>0.020</i>	k-range 3.5-9.5		
X6 Kloten	Cd–O	6	2.28 (0.01)	0.010 (0.000)	2.19 (0.63)	<i>0.90</i>	0.33
100 $\mu$ M Cd	Cd···C	<i>1.5</i>	3.16 (0.03)	0.012 (0.004)			
500 $\mu$ M P	Cd–O–O <sup>c</sup>	<i>18</i>	4.79 (0.05)	<i>0.020</i>	k-range 3.5-9.5		
pH 5.85					k-range 3.5-9.5		
X7 Kloten	Cd–O	6	2.27 (0.01)	0.012 (0.000)	1.92 (0.74)	<i>0.90</i>	0.33
100 $\mu$ M Cd	Cd···C	<i>1.5</i>	3.09 (0.04)	0.014 (0.004)			
500 $\mu$ M As	Cd–O–O <sup>c</sup>	<i>18</i>	4.65 (0.06)	<i>0.020</i>	k-range 3.5-9.5		
pH 6.15					k-range 3.5-9.5		
Y2 Risfallet	Cd–O	6	2.28 (0.01)	0.009 (0.000)	2.54 (0.78)	<i>0.90</i>	0.49
100 $\mu$ M Cd	Cd···C	<i>1.5</i>	3.15 (0.04)	0.013 (0.005)			
pH 5.64	Cd–O–O <sup>c</sup>	<i>18</i>	4.70 (0.06)	<i>0.019</i>	k-range 3.5-9.5		
Y7 Risfallet	Cd–O	6	2.28 (0.00)	0.009 (0.000)	2.11 (0.49)	<i>0.90</i>	0.20
100 $\mu$ M Cd	Cd···C	<i>1.5</i>	3.15 (0.02)	0.008 (0.002)			
500 $\mu$ M As	Cd–O–O <sup>b</sup>	<i>18</i>	4.73 (0.04)	<i>0.019</i>	k-range 3.5-9.5		
pH 6.15					k-range 3.5-9.5		
Cd(aq)	Cd–O	6	2.27 (0.006)	0.008 (0.000)	2.87 (0.58)	<i>0.65</i>	0.70
Cd(NO <sub>3</sub> ) <sub>2</sub>	Cd–O–O <sup>c</sup>	<i>18</i>	4.40 (0.033)	<i>0.017</i>	k-range 3-10		
0.5 M	Cd–O···O <sup>d</sup>	<i>24</i>	3.70 (0.10)	<i>0.025</i>	k-range 3-10		
Cd(aq)	Cd–O	6	2.27 (0.01)	0.008 (0.000)	0.70 (0.62)	<i>1</i>	0.66
Cd(NO <sub>3</sub> ) <sub>2</sub>	Cd–O–O <sup>c</sup>	<i>18</i>	4.43 (0.03)	<i>0.017</i>	k-range 3-10		
15 mM	Cd–O···O <sup>d</sup>	<i>24</i>	3.72 (0.10)	<i>0.025</i>	k-range 3-10		
Cd-FA	Cd–O	6	2.27 (0.005)	0.007 (0.000)	1.57 (0.64)	<i>0.80</i>	0.39
8 mM Cd	Cd···C	2	3.12 (0.03)	0.013 (0.04)			
8 g L <sup>-1</sup> FA	Cd–O–O <sup>c</sup>	<i>18</i>	4.67 (0.05)	<i>0.014</i>	k-range 3.4-10		
pH 6.32					k-range 3.4-10		

<sup>a</sup>CN = Coordination number; R = Atomic distance;  $\sigma^2$  = Debye-Waller factor;  $\Delta E$  = Energy shift parameter;  $S_0^2$  = Passive amplitude reduction factor; R=R-factor = goodness-of-fit parameter of the Fourier Transform; sum of the squares of the differences between the data and the fit at each data point, divided by the sum of the squares of the data at each corresponding point. In general, R-factor values less than 5% are considered to reflect a reasonable fit. Uncertainties of fitted parameters as given in Artemis (Ravel & Newville, 2005).

<sup>b</sup>Added concentrations of cadmium(II), phosphate and arsenate are listed below sample name.

<sup>c</sup>The  $\sigma^2$  (Å<sup>2</sup>) of Cd–O–O (multiple scattering paths) was defined as  $2*\sigma^2$  (Å<sup>2</sup>) for the Cd–O paths.

<sup>d</sup>For each sample the  $\sigma^2$  (Å<sup>2</sup>) of Cd–O···O (multiple scattering paths) was defined as  $3*\sigma^2$  (Å<sup>2</sup>) for the Cd–O paths.

## Conclusions

The main conclusions of this thesis can be summarised as follows:

- Phosphate increases the sorption of lead(II), copper(II) and cadmium(II) to ferrihydrite. In systems without phosphate, the metals are primarily adsorbed as inner-sphere bidentate complexes to the ferrihydrite surface. The increase in sorption due to phosphate cannot be explained solely by electrostatic interactions. Inclusion of ternary complexes consistent with EXAFS measurements into the CD-MUSIC model can successfully simulate the enhanced sorption. These ternary complexes include the metal ion, two surface groups and the phosphate ion.
- Phosphate is more strongly bound to surface sites on poorly crystalline aluminium hydroxide (Alhox) than on ferrihydrite. Phosphate is also more strongly adsorbed to Alhox than arsenate. Consequently, phosphate competes more strongly with arsenate for sorption sites on the surface of Alhox than on ferrihydrite.
- The effect of ZVI amendments on copper and arsenic solubility is long-lasting. Copper and arsenic are stabilised by inner-sphere complexation to iron (hydr)oxides 6 and 15 years after ZVI addition. Model simulations show that copper immobilisation is most effective at high pH (>6) and a low content of organic matter. Arsenate retention is less dependent on the pH value, but competition with phosphate must be taken into account in the model, as otherwise the sorption might be greatly overestimated.

- Addition of phosphate did not affect lead(II), copper(II) or cadmium(II) sorption to B- and C-horizons of podzolised soils at moderate levels of contaminants and phosphate. The reasons may be high binding to organic matter and low addition of phosphorus, *e.g.* binding to organic matter dominated cadmium speciation in two B-horizons studied here. This does not rule out that phosphate could increase sorption in soils with a higher content of iron (hydr)oxides compared with organic matter at higher additions of phosphate.

## Implications and future research

A better understanding of metal and arsenic sorption mechanisms in soils and other matrices improves the quality of risk assessments and enables a more cost-effective and safe design of remediation solutions. It also opens the way for development of modelling tools that can be used to understand and predict the fate of contaminants under different environmental conditions.

In the work presented in this thesis, phosphate greatly increased sorption of lead(II) and cadmium(II) to ferrihydrite, while copper(II) sorption was less affected. On the other hand, moderate phosphate additions did not affect the sorption of these metals in soil at moderate contamination levels. This implies, for example, that addition of phosphate in order to increase the fertility of a contaminated soil as part of a remediation option would not increase, but possibly decrease, the mobility of lead, copper and cadmium. Knowledge of the sorption mechanisms could also be utilised in development of reactive materials for remediation of contaminated soils or waters. The surface complexation model would be a valuable tool in such development work.

This thesis also showed that phosphate decreases the sorption of arsenate more on poorly crystalline aluminium hydroxide than on ferrihydrite. Consequently, care has to be taken when adding phosphate to arsenate-contaminated soils, especially soils rich in aluminium. More knowledge about the effects of phosphate on arsenate sorption/desorption in aluminium-rich soils is needed. It would be useful to parameterise hydroxy-aluminium and aluminosilicate minerals that are common in soils in the CD-MUSIC model, as well as assemblages of iron and aluminium minerals.

The geochemical model developed and used for scenario modelling in Paper III exemplifies the power of state-of-the-art geochemical models in the design of remediation solutions and prediction of contaminant mobility. A limiting factor in application of *in situ* technologies is often uncertainty about the long-term performance and the use of geochemical models can permit more

confident assessment. To assess other contaminants and stabilising amendments, new models need to be developed.

The overestimation of arsenate sorption in soil in the model simulation in Paper III highlights a knowledge gap. Interactions between iron and aluminium (hydr)oxides and organic matter are not described in the model. More insights into ageing effects of stabilised soils are also needed, *e.g.* concerning the extent to which contaminants are incorporated in the matrix or released. Explaining and quantifying these interactions and, if possible, including them in a geochemical model is an interesting area for future research.

## 6 References

- Anderson, P.R. & Benjamin, M.M. (1990). Surface and bulk characteristics of binary oxide suspensions. *Environmental Science & Technology*, 24(5), pp. 692-698.
- Antelo, J., Arce, F. & Fiol, S. (2015). Arsenate and phosphate adsorption on ferrihydrite nanoparticles. Synergetic interaction with calcium ions. *Chemical Geology*, 410, pp. 53-62.
- Antelo, J., Fiol, S., Perez, C., Marino, S., Arce, F., Gondar, D. & Lopez, R. (2010). Analysis of phosphate adsorption onto ferrihydrite using the CD-MUSIC model. *Journal of Colloid and Interface Science*, 347(1), pp. 112-119.
- Arai, Y., Elzinga, E.J. & Sparks, D.L. (2001). X-ray absorption spectroscopic investigation of arsenite and arsenate adsorption at the aluminum oxide-water interface. *Journal of Colloid and Interface Science*, 235(1), pp. 80-88.
- Arai, Y. & Sparks, D.L. (2001). ATR-FTIR spectroscopic investigation on phosphate adsorption mechanisms at the ferrihydrite-water interface. *Journal of Colloid and Interface Science*, 241(2), pp. 317-326.
- Arai, Y., Sparks, D.L. & Davis, J.A. (2005). Arsenate adsorption mechanisms at the allophane - Water interface. *Environmental Science and Technology*, 39(8), pp. 2537-2544.
- Benjamin, M.M. & Leckie, J.O. (1981). Multiple-site adsorption of Cd, Cu, Zn, and Pb on amorphous iron oxyhydroxide. *Journal of Colloid and Interface Science*, 79(1), pp. 209-221.
- Bes, C. & Mench, M. (2008). Remediation of copper-contaminated topsoils from a wood treatment facility using in situ stabilisation. *Environmental Pollution*, 156(3), pp. 1128-1138.
- Carabante, I., Grahn, M., Holmgren, A., Kumpiene, J. & Hedlund, J. (2009). Adsorption of As(V) on iron oxide nanoparticle films studied by in situ ATR-FTIR spectroscopy. *Colloids and Surfaces A: Physicochemical and Engineering Aspects*, 346(1-3), pp. 106-113.
- Collins, C.R., Ragnarsdottir, K.V. & Sherman, D.M. (1999). Effect of inorganic and organic ligands on the mechanism of cadmium sorption to goethite. *Geochimica et Cosmochimica Acta*, 63(19/20), pp. 2989-3002.

- Colombo, C. & Violante, A. (1996). Effect of time and temperature on the chemical composition and crystallization of mixed iron and aluminum species. *Clays and clay minerals*, 44(1), pp. 113-120.
- Communication from the Commission to the Council, the European Parliament, the European Economic and Social Committee and the Committee of the Regions - Thematic Strategy for Soil Protection [SEC(2006)620] [SEC(2006)1165]
- Cornell, R.M. & Schwertmann, U. (2003). *The iron oxides*. Second. Ed. Wiley-VCH, Weinheim.
- Cundy, A.B., Hopkinson, L. & Whitby, R.L.D. (2008). Use of iron-based technologies in contaminated land and groundwater remediation: A review. *Science of the Total Environment*, 400(1–3), pp. 42-51.
- Das, S., Hendry, M.J. & Essilfie-Dughan, J. (2011). Effects of adsorbed arsenate on the rate of transformation of 2-line ferrihydrite at pH 10. *Environmental Science & Technology*, 45(13), pp. 5557-5563.
- Davis, J.A. & Leckie, J.O. (1978). Surface ionization and complexation at the oxide/water interface II. Surface properties of amorphous iron oxyhydroxide and adsorption of metal ions. *Journal of Colloid and Interface Science*, 67(1), pp. 90-107.
- Del Nero, M., Galindo, C., Barillon, R., Halter, E. & Madé, B. (2010). Surface reactivity of  $\alpha$ -Al<sub>2</sub>O<sub>3</sub> and mechanisms of phosphate sorption: In situ ATR-FTIR spectroscopy and  $\zeta$  potential studies. *Journal of Colloid and Interface Science*, 342(2), pp. 437-444.
- Doherty, J. (2010). *PEST. Model-independent parameter estimation. User manual, 5th edition*. [Computer Program]. Web: <http://www.pesthomepage.org>: Watermark Numerical Computing.
- Dzombak, D.A. & Morel, F.M.M. (1990). *Surface complexation modeling - hydrous ferric oxide*. John Wiley and Sons, New York, USA.
- Elzinga, E.J. & Kretzschmar, R. (2013). In situ ATR-FTIR spectroscopic analysis of the co-adsorption of orthophosphate and Cd(II) onto hematite. *Geochimica et Cosmochimica Acta*, 117 (53-64).
- Elzinga, E.J., Peak, D. & Sparks, D.L. (2001). Spectroscopic studies of Pb(II)-sulfate interactions at the goethite-water interface. *Geochimica et Cosmochimica Acta*, 65(14), pp. 2219-2230.
- Garcia-Sanchez, A., Alvarez-Ayoso, E. & Rodrigues-Martin, F. (2002). Sorption of As(V) by some oxyhydroxides and clay minerals. Application to its immobilization in two polluted mining soils. *Clay Minerals*, 37, pp. 187-194.
- Goldberg, S. (2007). Adsorption-desorption processes in subsurface reactive transport modeling. *Vadose Zone Journal*, 6(3), pp. 407-435.
- Goldberg, S. (2002). Competitive adsorption of arsenate and arsenite on oxides and clay Minerals. *Soil Science Society of America Journal*, 66, pp. 413-421.
- Goldberg, S., Davis, J.A. & Hem, J.D. (1996). The surface chemistry of aluminum oxides and hydroxides. In: Sposito, G. (eds.) *The environmental chemistry of aluminum*. CRC Press, pp. 271-331, USA.
- Guan, X.-H., Liu, Q., Chen, G.-H. & Shang, C. (2005). Surface complexation of condensed phosphate to aluminum hydroxide: An ATR-FTIR

- spectroscopic investigation. *Journal of Colloid and Interface Science*, 289(2), pp. 319-327.
- Gustafsson, J.P. (2006). Arsenate adsorption to soils: Modelling the competition from humic substances. *Geoderma*, 136(1), pp. 320-330.
- Gustafsson, J.P. (2013). *Visual MINTEQ 3.1*, <http://vminTEQ.lwr.kth.se/>. [Computer program].
- Gustafsson, J.P. & Bhattacharya, P. (2007). Geochemical modelling of arsenic adsorption to oxide surfaces. In: Bhattacharya, P., Mukherjee, A.B., Bundschuh, J., Richard, H.L. (eds.) *Trace Metals and other Contaminants in the Environment*. (9) Elsevier, pp. 159-206. .
- Gustafsson, J.P., Bhattacharya, P. & Karlton, E. (1999). Mineralogy of poorly crystalline aluminium phases in the B horizon of Podzols in southern Sweden. *Applied Geochemistry*, 14(6), pp. 707-718.
- Gustafsson, J.P. & Van Schaik, J.W.J. (2003). Cation binding in a mor layer: batch experiments and modelling. *European Journal of Soil Science*, 54(2), pp. 295-310.
- Gustafsson, J.P. & Kleja, D.B. (2005). Modeling salt-dependent proton binding by organic soils with the NICA-Donnan and Stockholm Humic models. *Environmental Science & Technology*, 39(14), pp. 5372-5377.
- Gustafsson, J.P., Tiberg, C., Edkymish, A. & Kleja, D.B. (2011). Modelling lead(II) sorption to ferrihydrite and soil organic matter. *Environmental Chemistry*, 8(5), pp. 485-492
- Harvey, O.R. & Rhue, R.D. (2008). Kinetics and energetics of phosphate sorption in a multi-component Al(III)–Fe(III) hydr(oxide) sorbent system. *Journal of Colloid and Interface Science*, 322(2), pp. 384-393.
- Herbelin, A.L. & Westall, J.C. (1999). *FITEQL 4.0: A computer program for determination of chemical equilibrium constants from experimental data. Report 99-0a.*: Department of Chemistry, Oregon State University, Corvallis, USA.
- Hiemstra, T. (2013). Surface and mineral structure of ferrihydrite. *Geochimica et Cosmochimica Acta*, 105, pp. 316-325.
- Hiemstra, T. & van Riemsdijk, W.H. (1996). A surface structural approach to ion adsorption: The charge distribution (CD) model. *Journal of Colloid and Interface Science*, 179, pp. 488-508.
- Hiemstra, T. & Van Riemsdijk, W.H. (1999). Surface structural ion adsorption modeling of competitive binding of oxyanions by metal (hydr)oxides. *Journal of Colloid and Interface Science*, 210(1), pp. 182-193.
- Hiemstra, T. & Van Riemsdijk, W.H. (2009). A surface structural model for ferrihydrite I: Sites related to primary charge, molar mass, and mass density. *Geochimica et Cosmochimica Acta*, 73(15), pp. 4423-4436.
- Hopp, L., Nico, P.S., Marcus, M.A. & Peiffer, S. (2008). Arsenic and chromium partitioning in a podzolic soil contaminated by chromated copper arsenate. *Environmental Science & Technology*, 42(17), pp. 6481-6486.
- Huang, P.M., Wang, M.K., Kämpf, N. & Schulze, D.G. (2002). Chapter 8, Aluminum hydroxides. In: Dixon, J.B. & Schulze, D.G. (eds) *Soil mineralogy with environmental applications*. Madison, US: Soil Science Society of America Inc., pp. 261-289.

- Jambor, J.L. & Dutrizac, J.E. (1998). Occurrence and constitution of natural and synthetic ferrihydrite, a widespread iron oxyhydroxide. *Chemical Reviews*, 98(7), pp. 2549-2585.
- Johnston, C.P. & Chrysochoou, M. (2016). Mechanisms of Chromate, selenate, and sulfate adsorption on Al-Substituted ferrihydrite: implications for ferrihydrite surface structure and reactivity. *Environmental Science & Technology* Article ASAP.
- Karlsson, T., Persson, P. & Skyllberg, U. (2005). Extended X-ray absorption fine structure spectroscopy evidence for the complexation of cadmium by reduced sulfur groups in natural organic matter. *Environmental Science & Technology*, 39(9), pp. 3048-3055.
- Karlsson, T., Persson, P. & Skyllberg, U. (2006). Complexation of copper(II) in organic soils and in dissolved organic matter – EXAFS evidence for chelate ring structures. *Environmental Science & Technology*, 40(8), pp. 2623-2628.
- Kelly, S., Hesterberg, D. & Ravel, B. (2008). Analysis of soils and minerals using X-ray absorption spectroscopy. In: Ulery, A.L. & Drees, R.L. (eds) *Methods of soil analysis. Part 5. Mineralogical methods*. SSSA Book Series, SSSA, Madison, WI, USA, pp. 387-464.
- Komarek, M., Vanek, A. & Ettler, V. (2013). Chemical stabilization of metals and arsenic in contaminated soils using oxides - A review. *Environmental Pollution*, 172, pp. 9-22.
- Kumpiene, J., Castillo Montesinos, I., Lagerkvist, A. & Maurice, C. (2007). Evaluation of the critical factors controlling stability of chromium, copper, arsenic and zinc in iron-treated soil. *Chemosphere*, 67(2), pp. 410-417.
- Kumpiene, J., Lagerkvist, A. & Maurice, C. (2008). Stabilization of As, Cr, Cu, Pb and Zn in soil using amendments – a review. *Waste Management*, 28(1), pp. 215-225.
- Kumpiene, J., Ore, S., Renella, G., Mench, M., Lagerkvist, A. & Maurice, C. (2006). Assessment of zerovalent iron for stabilization of chromium, copper, and arsenic in soil. *Environmental Pollution*, 144(1), pp. 62-69.
- Liu, Y.-T. & Hesterberg, D. (2011). Phosphate bonding on noncrystalline Al/Fe-hydroxide coprecipitates. *Environmental Science & Technology*, 45(15), pp. 6283-6289.
- Loring, J.S., Sandström, M.H., Norén, K. & Persson, P. (2009). Rethinking arsenate coordination at the surface of goethite. *Chemistry – A European Journal*, 15(20), pp. 5063-5072.
- Manceau, A. (1995). The mechanism of anion adsorption on iron oxides: Evidence for the bonding of arsenate tetrahedra on free Fe(O, OH)<sub>6</sub> edges. *Geochimica et Cosmochimica Acta*, 59(17), pp. 3647–3653.
- Manning, B. (2005). Arsenic speciation in As(III)- and As(V)-treated soil using XANES spectroscopy. *Microchimica Acta*, 151(3-4), pp. 181-188.
- Manning, B.A. & Goldberg, S. (1996). Modeling competitive adsorption of arsenate with phosphate and molybdate on oxide minerals. *Soil Science Society of America Journal*, 60(1), pp. 121-131.

- Martin, M., Violante, A., Ajmone-Marsan, F. & Barberis, E. (2014). Surface interactions of arsenite and arsenate on soil colloids. *Soil Science Society of America Journal*, 78(1) pp. 157-170.
- Masue, Y., Loeppert, R.H. & Kramer, T.A. (2007). Arsenate and arsenite adsorption and desorption behavior on coprecipitated aluminum: iron hydroxides. *Environmental Science & Technology*, 41(3), pp. 837-842.
- Mench, M., Vangronsveld, J., Beckx, C. & Ruttens, A. (2006). Progress in assisted natural remediation of an arsenic contaminated agricultural soil. *Environmental Pollution*, 144(1), pp. 51-61.
- Michel, F.M., Barron, V., Torrent, J., Morales, M.P., Serna, C.J., Boily, J.F., Liu, Q.S., Ambrosini, A., Cismasu, A.C. & Brown, G.E. (2010). Ordered ferrimagnetic form of ferrihydrite reveals links among structure, composition, and magnetism. *Proceedings of the National Academy of Sciences of the United States of America*, 107(7), pp. 2787-2792.
- Michel, F.M., Ehm, L., Antao, S.M., Lee, P.L., Chupas, P.J., Liu, G., Strongin, D.R., Schoonen, M.A.A., Phillips, B.L. & Parise, J.B. (2007). The structure of ferrihydrite, a nanocrystalline material. *Science*, 316(5832), pp. 1726-1729.
- Mohan, D. & Pittman Jr, C.U. (2007). Arsenic removal from water/wastewater using adsorbents—A critical review. *Journal of Hazardous Materials*, 142(1–2), pp. 1-53.
- Mähler, J., Persson, I. & Herbert, R.B. (2013). Hydration of arsenic oxyacid species. *Dalton Transactions*, 42(5), pp. 1364-1377.
- Nelson, H., Sjöberg, S. & Lövgren, L. (2013). Surface complexation modelling of arsenate and copper adsorbed at the goethite/water interface. *Applied Geochemistry*, 35, pp. 696-704.
- Ostergren, J.D., Brown, G.E., Parks, G.A. & Persson, P. (2000). Inorganic ligand effects on Pb(II) sorption to goethite ( $\alpha$ -FeOOH) - II. Sulfate. *Journal of Colloid and Interface Science*, 225(2), pp. 483-493.
- Parkman, R.H., Charnock, J.M., Bryan, N.D., Livens, F.R. & Vaughan, D.J. (1999). Reactions of copper and cadmium ions in aqueous solution with goethite, lepidocrocite, mackinawite, and pyrite. *American Mineralogist*, 84(3), pp. 407-419.
- Peacock, C.L. & Sherman, D.M. (2004). Copper(II) sorption onto goethite, hematite and lepidocrocite: A surface complexation model based on ab initio molecular geometries and EXAFS spectroscopy. *Geochimica et Cosmochimica Acta*, 68(12), pp. 2623-2637.
- Pearson, R.G. (1963). Hard and Soft Acids and Bases. *Journal of the American Chemical Society*, 85(22), pp. 3533-3539.
- Persson, P., Nilsson, N. & Sjöberg, S. (1996). Structure and bonding of orthophosphate ions at the iron oxide–aqueous interface. *Journal of Colloid and Interface Science*, 177(1), pp. 263-275.
- Ponthieu, M., Juillot, F., Hiemstra, T., van Riemsdijk, W.H. & Benedetti, M.F. (2006). Metal ion binding to iron oxides. *Geochimica et Cosmochimica Acta*, 70(11), pp. 2679-2698.

- Randall, S.R., Sherman, D.M., Ragnarsdottir, K.V. & Collins, C.R. (1999). The mechanism of cadmium surface complexation on iron oxyhydroxide minerals. *Geochimica et Cosmochimica Acta*, 63(19-20), pp. 2971-2987.
- Ravel, B. & Newville, M. (2005). ATHENA, ARTEMIS, HEPHAESTUS: data analysis for X-ray absorption spectroscopy using IFEFFIT. *Journal of Synchrotron Radiation*, 12, pp. 537-541.
- Scheinost, A.C., Abend, S., Pandya, K.I. & Sparks, D.L. (2001). Kinetic controls on Cu and Pb sorption by ferrihydrite. *Environmental Science & Technology*, 35, pp. 1090-1096.
- Schwertmann, U. & Cornell, R.M. (2000). *Iron oxides in the laboratory: preparation and characterization*. Wiley: Weinheim, Germany.
- SGU (2013). Bedömningsgrunder för grundvatten. *SGU Rapport*, Uppsala, Sweden.
- Sheals, J., Granström, M., Sjöberg, S., Persson, P. (2003). Coadsorption of Cu(II) and glyphosate at the water-goethite ( $\alpha\text{FeOOH}$ ) interface: molecular structures from FTIR and EXAFS measurements. *Journal of Colloid and Interface Science*, 262, pp. 38-47.
- Sherman, D.M. & Randall, S.R. (2003). Surface complexation of arsenic(V) to iron(III) (hydr)oxides: structural mechanism from ab initio molecular geometries and EXAFS spectroscopy. *Geochimica et Cosmochimica Acta*, 67(22), pp. 4223-4230.
- Sjöstedt, C., Wällstedt, T., Gustafsson, J.P. & Borg, H. (2009). Speciation of aluminium, arsenic and molybdenum in excessively limed lakes. *Science of the Total Environment*, 407(18), pp. 5119-5127.
- Spadini, L., Manceau, A., Schindler, P.W. & Charlet, L. (1994). Structure and stability of  $\text{Cd}^{2+}$  surface complexes on ferric oxides: 1. Results from EXAFS spectroscopy. *Journal of Colloid and Interface Science*, 168(1), pp. 73-86.
- Spadini, L., Schindler, P.W., Charlet, L., Manceau, A. & Ragnarsdottir, K.V. (2003). Hydrated ferric oxide: evaluation of Cd-HFO surface complexation models combining Cd K EXAFS data, potentiometric titration results, and surface site structures identified from mineralogical knowledge. *Journal of Colloid and Interface Science*, 266(1), pp. 1-18.
- Stegemeier, J.P., Reinsch, B.C., Lentini, C.J., Dale, J.G. & Kim, C.S. (2015). Aggregation of nanoscale iron oxyhydroxides and corresponding effects on metal uptake, retention, and speciation: II. Temperature and time. *Geochimica et Cosmochimica Acta*, 148(0), pp. 113-129.
- Strawn, D.G. & Baker, L.L. (2009). Molecular characterization of copper in soils using X-ray absorption spectroscopy. *Environmental Pollution*, 157(10), pp. 2813-2821.
- Suresh Kumar, P., Flores, R.Q., Sjöstedt, C. & Önnby, L. (2016). Arsenic adsorption by iron-aluminium hydroxide coated onto macroporous supports: Insights from X-ray absorption spectroscopy and comparison with granular ferric hydroxides. *Journal of Hazardous Materials*, 302, pp. 166-174.
- Swedish Environmental Protection Agency (2002). *Methods for inventories of contaminated sites, Report 5053, 1<sup>st</sup> edition*. Värnamo, Sweden.

- Swedlund, P.J., Holtkamp, H., Song, Y.T. & Daughney, C.J. (2014). Arsenate-ferrihydrite systems from minutes to months: a macroscopic and IR spectroscopic study of an elusive equilibrium. *Environmental Science & Technology*, 48(5), pp. 2759-2765.
- Swedlund, P.J. & Webster, J.G. (2001). Cu and Zn ternary surface complex formation with SO<sub>4</sub> on ferrihydrite and schwertmannite. *Applied Geochemistry*, 16(5), pp. 503-511.
- Swedlund, P.J., Webster, J.G. & Miskelly, G.M. (2003). The effect of SO<sub>4</sub> on the ferrihydrite adsorption of Co, Pb and Cd: ternary complexes and site heterogeneity. *Applied Geochemistry*, 18(11), pp. 1671-1689.
- Tejedor-Tejedor, M.I. & Anderson, M.A. (1990). The protonation of phosphate on the surface of goethite as studied by CIR-FTIR and electrophoretic mobility. *Langmuir*, 6(3), pp. 602-611.
- Thompson, A., Attwood, D., Gullikson, E., Howells, M., Kim, K.-J., Kirtz, J., Kortright, J., Lindau, I., Liu, Y., Pianetta, P., Robinson, A., Scofield, J., Underwood, J., Williams, G. & Winck, H. (2009). *X-ray data booklet*. Berkeley, California: Lawrence Berkeley National Laboratory, University of California, USA.
- Trivedi, P., Dyer, J.A., Sparks, D.L., (2003). Lead sorption onto ferrihydrite. 1. A macroscopic and spectroscopic assessment. *Environmental Science & Technology*, 37, pp. 908-914.
- van Liedekerke, M., Prokop, G., Rabl-Berger, S., Kibblewhite, M. & Louwagie, G. (2014). *Progress in the management of Contaminated Sites in Europe*. JRC Reference reports. Luxembourg: Joint Research Centre of the European Commission.
- van Reeuwijk, L.P. (1995). *Procedures for Soil Analyses*. International Soil Reference and Information Centre, Wageningen, Netherlands.
- Venema, P., Hiemstra, T. & vanRiemsdijk, W.H. (1997). Interaction of cadmium with phosphate on goethite. *Journal of Colloid and Interface Science*, 192(1), pp. 94-103.
- Vermeer, A.W.P., van Riemsdijk, W.H. & Koopal, L.K. (1998). Adsorption of humic acid to mineral particles. 1. Specific and electrostatic interactions. *Langmuir*, 14(10), pp. 2810-2819.
- Violante, A. & Pigna, M. (2002). Competitive sorption of arsenate and phosphate on different clay minerals and soils. *Soil Science Society of America Journal*, 66(6), pp. 1788-1796.
- Vu, H.P., Shaw, S., Brinza, L. & Benning, L.G. (2013). Partitioning of Pb(II) during goethite and hematite crystallization: Implications for Pb transport in natural systems. *Applied Geochemistry*, 39, pp. 119-128.
- Wang, K. & Xing, B. (2002). Adsorption and desorption of cadmium by goethite pretreated with phosphate. *Chemosphere*, 48(7), pp. 665-670.
- Waychunas, G.A., Rea, B.A., Fuller, C.C. & Davis, J.A. (1993). Surface chemistry of ferrihydrite: Part 1. EXAFS studies of the geometry of coprecipitated and adsorbed arsenate. *Geochimica et Cosmochimica Acta*, 57(10), pp. 2251-2269.

- Weesner, F.J. & Bleam, W.F. (1998). Binding characteristics of  $Pb^{2+}$  on anion-modified and pristine hydrous oxide surfaces studied by electrophoretic mobility and X-ray absorption spectroscopy. *Journal of Colloid and Interface Science*, 205(2), pp. 380-389.
- Xiao, F., Wang, S., Xu, L., Wang, Y., Yuan, Z. & Jia, Y. (2015). Adsorption of monothioarsenate on amorphous aluminum hydroxide under anaerobic conditions. *Chemical Geology*, 407–408(0), pp. 46-53.
- Xie, L. & Giammar, D.E. (2007). Influence of phosphate on adsorption and surface precipitation of lead on iron oxide surfaces. In: Barnett, M. O., and Kent, D. B. (eds.) *Adsorption of Metals by Geomedia II: Variables, Mechanisms and Model Applications* Elsevier, Amsterdam, Netherlands, pp. 349–373.

## 7 Acknowledgements

I am grateful to the department of Soil and Environment at SLU and the Geological Survey of Sweden, SGU, for funding my PhD project. In addition, the Swedish Geotechnical Institute, SGI, supported part of the project.

Important parts of this research were performed at synchrotrons. My sincere thanks for allotted beamtime and support by beamline staff at beamline 4-1, Stanford Synchrotron Radiation Lightsource (SSRL) in the US, beamline X-11A at the National Synchrotron Lightsource (NSLS) also the US, beamline B18 at the Diamond Lightsource in the UK, beamline 8, Synchrotron Light Research Institute, Thailand, and last but not least beamline I811 at MAX-lab in Sweden.

I want to thank my supervisors for the privilege to do this PhD project, I am truly grateful that I got this opportunity! First, to my main supervisor Jon Petter Gustafsson: thanks for support and guidance and for sharing knowledge, especially on geochemical modelling. Thanks to my co-supervisor Ingmar Persson for teaching me XAS data collection and analysis. That was essential for this work. Thanks to my co-supervisor Dan Berggren Kleja for your positive attitude and good advice on many different subjects. Finally, thanks to Carin Sjöstedt who was my fellow PhD student in the beginning and my co-supervisor in the end.

There are many people I could thank for advice, discussions and inspiration during these years. People I met at SLU or conferences, workshops, courses and synchrotrons. I cannot list them all but I especially want to thank all my fellow PhD students at SLU for support, laughs and discussions. You made the time at SLU really enjoyable and I will miss you all. I have shared a large part of my PhD time as well as my scientific interests with my colleagues Ann Kristin Eriksson, Maja Larsson, Carin Sjöstedt and Åsa Löv. Thanks for friendship and scientific discussions. We'll certainly keep in touch!

I also want to express my gratitude to Magnus Simonsson and Jan Eriksson for reviewing the thesis. Thanks to Bertil Nilsson, Lena Ek, Mirsada Kulenovic, Aidin Geranmayeh and Aleksandra Marsz for help with laboratory work.

Thanks to SGI, where I have also been employed during my time as a PhD student. Special thanks to the heads of my department at SGI during this period: David Bendz, Yvonne Rogbeck and Maria Carling, for making it possible to combine my PhD project with working at SGI. Thanks also to my fellow employees at SGI. I look forward to spend more time at the SGI office in Stockholm.

Thanks to my husband, Michael, for never ending love and support and for patience, especially during these last months of hard work. Thanks to my kids Flora and Axel for being wonderful and curious, occasionally teasing me for speaking “Earthish”.

Thanks to the extended family, especially my parents Eva and Tomas and parents-in-law Eva and Bo-Anders for their periodical assistance with the household. We have really appreciated your help! Thanks also to Danne for helping out on different occasions. Finally, thanks to my dear sisters Anna and Cecilia and to grandma Margit.